

AD-A067 164

MASSACHUSETTS INST OF TECH LEXINGTON LINCOLN LAB
GAINAS AND GAINASP MBE CRYSTAL GROWTH. (U)
APR 78 A R CALAWA

F/G 20/12

UNCLASSIFIED

ESD-TR-78-397

F19628-78-C-0002
NL

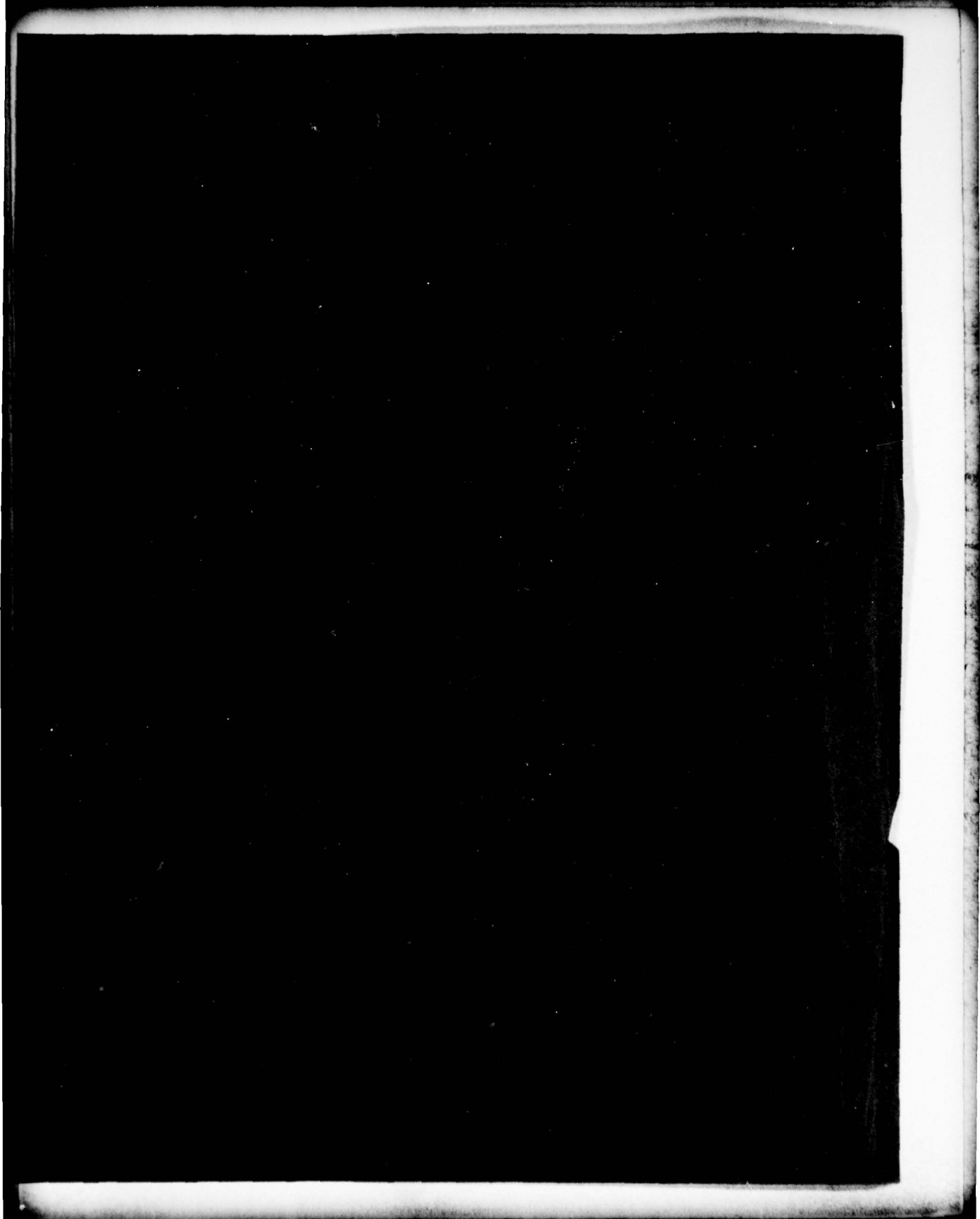
| OF |
AD
A087164



END
DATE
FILMED
8-79
DDC

DDC FILE COPY

AD A0 67 1 64



12

MASSACHUSETTS INSTITUTE OF TECHNOLOGY
LINCOLN LABORATORY

GaInAs AND GaInAsP MBE CRYSTAL GROWTH

DDC
RECEIVED
APR 10 1979
C

ANNUAL REPORT
TO THE
AIR FORCE OFFICE OF SCIENTIFIC RESEARCH

1 MAY 1977 - 30 APRIL 1978

Approved for public release; distribution unlimited.

LEXINGTON

MASSACHUSETTS

79 04 06 009

ABSTRACT

The most important result of the first year of this program is our discovery that the introduction of hydrogen during the growth of GaAs films by molecular beam epitaxy (MBE) brings about a dramatic improvement in the electrical characteristics of these films. In addition to providing a major advance in the growth of MBE GaAs, this technique should be very helpful in the growth of similarly high quality GaInAs and GaInAsP films on InP substrates, the long range goals of this program.

In addition to discovering, understanding, and optimizing the hydrogen growth technique, we have also grown GaInAs films on InP substrates, and have considered possible techniques for controlling the As to P ratio for GaInAsP layer growth.

Prior to the development of the hydrogen technique, several growths of GaAs on GaAs were completed in order to identify and eliminate sources of impurities from the MBE system. For n-type layers with carrier concentrations in excess of 10^{17} cm^{-3} the electrical characteristics appeared normal but as the carrier concentration was reduced below 10^{17} cm^{-3} the increase in 77 K mobility normally observed was not seen. This is expected if the ionized impurity concentration remains in the range of $5 \times 10^{16} \text{ cm}^{-3}$ to 10^{17} cm^{-3} . After a careful review of the literature,¹⁻⁸ it became apparent that very little 77 K mobility data on MBE layers was available and that nearly all of the published data agreed with our results.⁷ Only one published 77 K mobility value¹ was significantly higher than all the others and there is no indication of its reproducibility. This large number of compensating impurities would significantly reduce the electron drift velocity in these materials, an effect which is detrimental to microwave devices. The use of hydrogen during growth, described in detail in this report, significantly reduces the carrier compensation due to residual impurities and results in much higher electron mobilities. Results of photoluminescence measurements on these materials are given which tentatively identify the important residual impurities in MBE grown GaAs as due to carbon and oxygen.

In addition to the development of GaAs MBE growth, we have begun development of GaInAs growth and initial results of the growth of GaInAs layers on InP substrates are given. In particular, procedures are described by which uniform, homogeneous layers of GaInAs can be grown over large area substrates by precisely controlling the In/Ga ratio. Finally, consideration is given to the control of the As/P ratio for the MBE growth of GaInAsP on InP substrates.

ACCESSION for	
NTIS	Write Section <input checked="" type="checkbox"/>
DOC	B + Section <input type="checkbox"/>
UNANNOUNCED	<input type="checkbox"/>
JUSTIFIED	
BY	
DISTRIBUTION/AVAILABILITY NOTES	
1	SPECIAL
A	

CONTENTS

Abstract	iii
I. INTRODUCTION	1
II. PROGRESS DURING CURRENT PROGRAM YEAR	7
A. MBE System Description	7
B. Substrate Preparation	9
C. Electron Diffraction Studies	15
D. Mass Spectrum Analysis	21
E. Epitaxial Growth Parameters	23
F. Electrical Properties	25
G. Effect of H ₂ on Electrical Properties	25
H. Photoluminescence Measurements	33
I. Growth of In _{1-x} Ga _x As on InP	37
III. SUMMARY	40
IV. REFERENCES	41
V. BIOGRAPHY AND PUBLICATIONS OF PRINCIPAL INVESTIGATOR	44

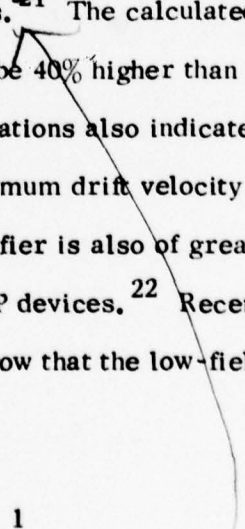


I. INTRODUCTION

The use of epitaxial layers and of heteroepitaxial layers of compound semiconductors in recent years has had a significant impact on the development of new and useful semiconductor devices. ^{1, 9-14}

Interest in the quaternary alloy $\text{Ga}_{1-x}\text{In}_x\text{As}_{1-y}\text{P}_y$ is primarily based on the applications of this material to optical devices such as light emitting diodes (LED), photo-emissive cathodes and heterojunction lasers. ¹⁵⁻¹⁸ The principal advantages of this material are that lattice-matched layers can be epitaxially grown on InP over a wide composition range, which permits the light emission of lasers and LEDs to be extended to longer wavelengths where optical fiber transmission is optimal. (Current state-of-the-art optical fibers have their best characteristics -- minimum loss ¹⁹ and minimum dispersion ²⁰ -- in the 1.1- to 1.3- μm range.) It is also of importance in electrooptical device applications that GaInAsP is lattice-matched to a binary compound substrate (InP), which is transparent at the operating wavelength of the devices.

The potential importance of these materials in microwave devices such as the metal-epitaxial semiconductor field-effect transistor (MESFET) and transferred electron devices is demonstrated in a comparison of the electron velocity-field characteristics of these alloys and of GaAs. ²¹ The calculated maximum electron drift velocity for the quaternary alloy can be 40% higher than for GaAs with a comparable high-field saturation velocity. Calculations also indicate that electrons in the ternary alloy $\text{Ga}_{0.5}\text{In}_{0.5}\text{As}$ have a maximum drift velocity about 15% greater than for GaAs. The transferred electron amplifier is also of great interest because of the observation of low noise figures for InP devices. ²² Recent experiments on the epitaxial growth of $\text{Ga}_{1-x}\text{In}_x\text{As}$ on GaAs show that the low-field mobilities for electrons



in these alloys increase monotonically from about $7,000 \text{ cm}^2/\text{Vsec}$ for GaAs²³ to $16,700 \text{ cm}^2/\text{Vsec}$ for InAs in spite of the lattice mismatch condition throughout the alloy range.²⁴ One of these ternary alloys ($\text{Ga}_{0.47}\text{In}_{0.53}\text{As}$) is lattice matched to InP and should be a good candidate for the study of MESFETs as well as avalanche photodiodes and heterostructure lasers. Furthermore, since the highest frequency devices require thin layers and controlled carrier concentration profiles, MBE is an excellent candidate for the growth of the active layers in these devices.

Many heterostructure devices have suffered substantial degradation in operation. Although the sources of this degradation are not well understood, in many cases there has been a correlation between the degradation and the propagation of defects in the epitaxial layers.²⁵ Three important sources of these defects are lattice-mismatch between layers, interface states, and the propagation of dislocations from the substrates. The first source of defects can be eliminated by growing lattice-matched epitaxial layers on single-crystal substrates, for example, GaInAsP on InP. We believe that layer growth by MBE has the potential to greatly reduce (and perhaps eliminate) the other two major sources of defects. Since the growth takes place in an ultra-high vacuum, it can be initiated onto either a congruently subliming substrate or a stoichiometrically stable substrate (e. g., for InP heated in a phosphorus environment), which should virtually eliminate terminal surface bonds or interface states. It has already been demonstrated²⁶ in GaAs that substrate surface asperities can be eliminated in the initial phase of MBE growth and atomically flat surfaces can be achieved. Also, since the substrate temperature required for proper MBE growth is lower than for other techniques, it may be possible to inhibit propagation of substrate dislocations.

Furthermore, it has been shown²⁷ that the thicknesses can be precisely controlled down to layers as thin as 50 Å and that the carrier concentration profiles can be abruptly and reproducibly changed within a few hundred angstroms.²⁸ This control has not been demonstrated with any other growth technique. We believe that the advancement of MBE technology will open a completely new era in semiconductor device technology.

MBE grown layers have been used to fabricate several semiconductor devices.²⁹⁻³⁸ Some of these devices are listed in Table I. The characteristics of these devices are comparable to those made from crystals grown by other techniques, which indicates that although MBE growth is a relatively new development, MBE technology is considerably advanced. We believe, however, that the discoveries which were made in the first year of this contract represent a significant contribution in the state of the art of GaAs MBE technology which will carry over to other III-V compounds and alloys. Further development is needed in the doping of MBE films without compensation of impurities. At the highest possible MBE growth rates of 3 Å/sec to 10 Å/sec the vapor pressure required to keep an unwanted impurity at a level of 10^{14} cm^{-3} would be about 10^{-15} Torr if we assume its sticking coefficient is unity. Fortunately, the most probably impurities, carbon and oxygen, are present in the vacuum system as gaseous compounds such as C_xH_y , CO, CO_2 and O_2 which are likely to have small sticking coefficients. However, most of these gases are present in the 10^{-10} Torr range and collide with the growth surface at about 10^{-3} times the incident gallium flux. If their lifetimes on the surface are sufficient for the molecules to reach their dissociation energy at the substrate growth temperature, then atoms such as carbon would probably be incorporated in the film. We believe that these effects are important and in fact are the limiting factors in current MBE film

TABLE I
SEMICONDUCTOR DEVICES MADE FROM MBE LAYERS

MATERIAL	DEVICE	INITIAL RESULTS	REFERENCE
GaAs - Al _x Ga _{1-x} As	DH LASER	CW UP TO 400°K $I_{th}^{300K} = 3.3 \times 10^3 \text{ A/cm}^2$	CHO, DIXON, CASEY, HARTMAN ¹⁹
GaAs	FET	NOISE FIGURE = 1.9 dB ASSOCIATED GAIN = 11 dB @ 6 GHz	CHO, DILORENZO, HEWITT, ²⁰ NIEHAUS, SCHLOSSER
GaAs	MIXER DIODE	CONVERSION LOSS 5.3 dB @ 51.5 GHz 8.5 dB @ 103 GHz CUT OFF FREQ. = 500 GHz	BALLAMY, CHO ²¹
GaAs	IMPATT DIODE	LO-HI-LO PROFILE POWER = 3.2 W @ 11.7 GHz EFF. = 18%	CHO, BALLAMY, DUNN, KUVAS, SCHROEDER ²²
GaAs - Al _{0.3} Ga _{0.7} As	INTERFERENCE FILTERS QUARTER WAVE STACKS WAVEGUIDE	BANDWIDTH 300 - 900 Å 15 LAYER REFLECTANCE @ 1.5 μm > 99% LOSS ≤ 1.5 cm ⁻¹ (0.89 - 1.1 μm)	VANDERZIEL, ILEGEMS ²³
Al _x Ga _{1-x} As	TAPERED COUPLER	EFFICIENCY ≈ 100%	MERZ, CHO ²⁴
GaAs - Al _x Ga _{1-x} As	DH LASER	CW UP TO 114°K TUNABLE FROM 8.54 TO 15.9 μm	MERZ, LOGAN, WIEGMANN, GOSSARD ²⁵
PbTe - Pb _{0.78} Sn _{0.22} Te	WAVEGUIDE	LOSS ≤ 1.5 cm ⁻¹ (10.6 μm)	WALPOLE, CALAWA, HARMAN, GROVES ²⁶
PbTe - Pb _{0.88} Sn _{0.12} Te	DFB LASER	CW UP TO 50°K SINGLE MODE TUNING = 7 cm ⁻¹	RALSTON, WALPOLE HARMAN, MELNGAILIS ²⁷ WALPOLE, CALAWA CHINN, GROVES, HARMAN ²⁸

quality. The pressure of these gases can be further reduced, possibly to 10^{-11} or 10^{-12} Torr, through cryogenic (10 K - 20 K) pumping. Such pumping will soon be incorporated into our system, but the times required to reach these partial pressures may be prohibitive. Even if these low partial pressures can be achieved, we believe that our current approach of reactively forming other compounds with the residual gases that neither stick nor remain dissociated at the growth interface will be beneficial in the growth of high quality epitaxial layers. To our knowledge, our research is the only work reported³⁹ on the doping effects of residual gases in MBE systems.

CT-95-277

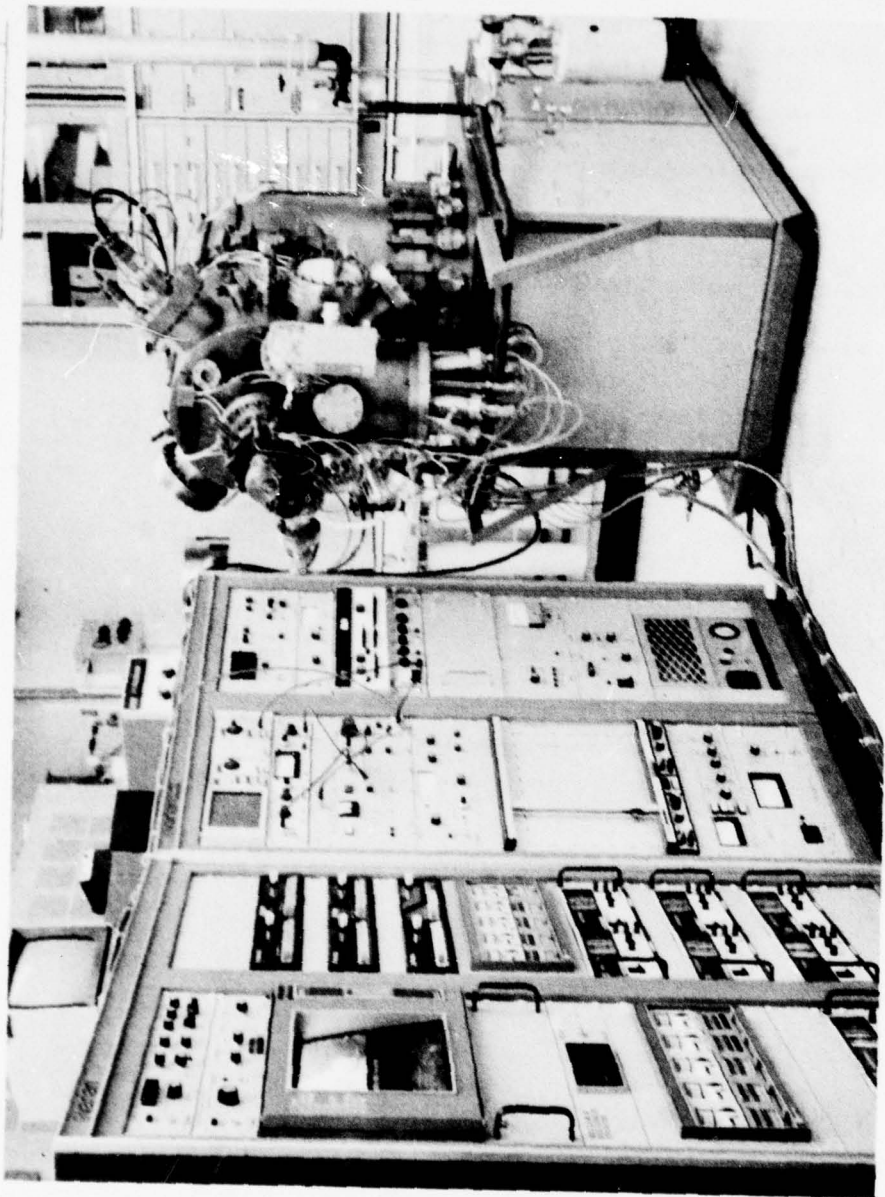


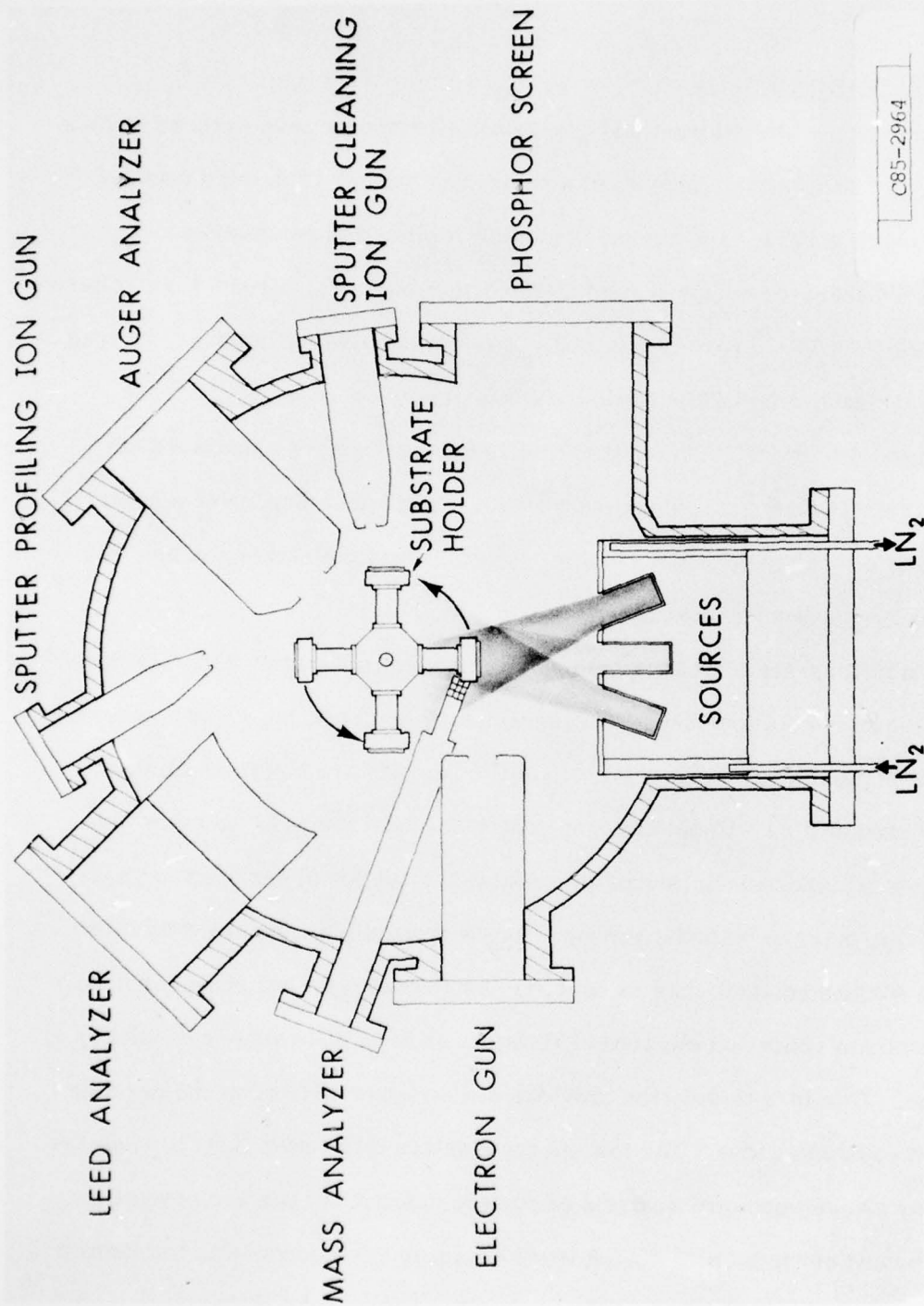
Fig. 1. Photograph of molecular-beam epitaxial growth system.

II. PROGRESS DURING CURRENT PROGRAM YEAR

A. MBE System Description:

A photograph of the MBE system and associated electronics used in these studies is shown in Fig. 1. The system consists of a horizontal bell jar ultra-high vacuum chamber pumped with a 400 l/s ion pump, a titanium sublimation pump and a LN₂ cryopump. After baking the entire system at 200°C for 24 hours, a room temperature system pressure of 2×10^{-10} Torr is attained. It is not necessary, however, to bake the system between each run. While loading the samples in the system, the work chamber is purged with dry N₂. The system can then be pumped to a pressure of 2×10^{-9} Torr within 16 hours. The dominant residual gas remaining is N₂ which has no apparent effect on the epitaxial growth. Several sample changes can be made before system baking again becomes necessary.

A schematic cross-section of the MBE work chamber is shown in Fig. 2. The substrates are mounted on a four-position carousel-type holder which is 360° rotatable and X, Y, Z translatable over about one cu. in. The sources are modified Knudsen cells and are surrounded by a liquid nitrogen cooled shroud. The MBE chamber also contains an Auger analyzer which is used to examine the substrate surfaces for possible contamination prior to epitaxial growth. Argon sputter ion guns are available to remove such surface contaminants as carbon. An electron gun and phosphor screen are provided to obtain reflection electron diffraction, (RED), patterns of the epitaxially growing surface. This in-situ detector provides a continuous monitor of the crystal-line quality of the epitaxial film. The low energy electron diffraction (LEED) analyzer is available for a two dimensional analysis of surface defects and surface crystallinity of the substrates and of the MBE films. A mass analyzer is also available to monitor the molecular beams and for analysis of the residual gases in the system.



C85-2964

Fig. 2. Cross-sectional sketch of molecular-beam epitaxial growth chamber showing arrangement of substrate holders, sources and surface analysis equipment.

A sectional sketch of our MBE source heater assembly is shown in Fig. 3. The entire assembly is made of 4 - 9's purity tantalum and pyrolytic boron nitride insulators. The source crucible (not shown in Fig. 3) is also made of high purity pyrolytic boron nitride.

The substrate holder assembly is shown in Fig. 4. The substrate is mounted with indium on the holder sub-assembly in a laminar flow clean bench. A cover glass is placed over the substrate to prevent particulate contamination in the transfer of the sub-assembly to the MBE chamber. The sub-assembly which now consists of the substrate indium --bonded to a M_0 disk and capped with a cover glass-- is also bonded with indium to the substrate holder to insure thermal uniformity. After evacuation of the MBE chamber, the cover glass is removed by rotating the substrate holder to the inverted position.

B. Substrate Preparation:

Although substrate preparation is important in any epitaxial growth process, it is probably more important in MBE growth than in any other. The reason for this is the lack of a convenient in-situ etch-back technique such as the melt-back technique in LPE and the vapor-etch technique in VPE which can uniformly remove several microns of surface damage due to handling.

It is possible that ion sputter etching could serve this purpose but it would be necessary to establish conditions for rapid uniform sputtering and to determine if there exist ion molecular species and energies at which these ions would stoichiometrically sputter the substrate surface. The stoichiometry must also be maintained in the post-annealing of the sputtering damage. To our knowledge there has been no careful study of sputter etching for MBE growth. The extent of ion sputter etching used in this study has been to clean the surface of carbon contamination which is believed to be within a few monolayers of the surface.

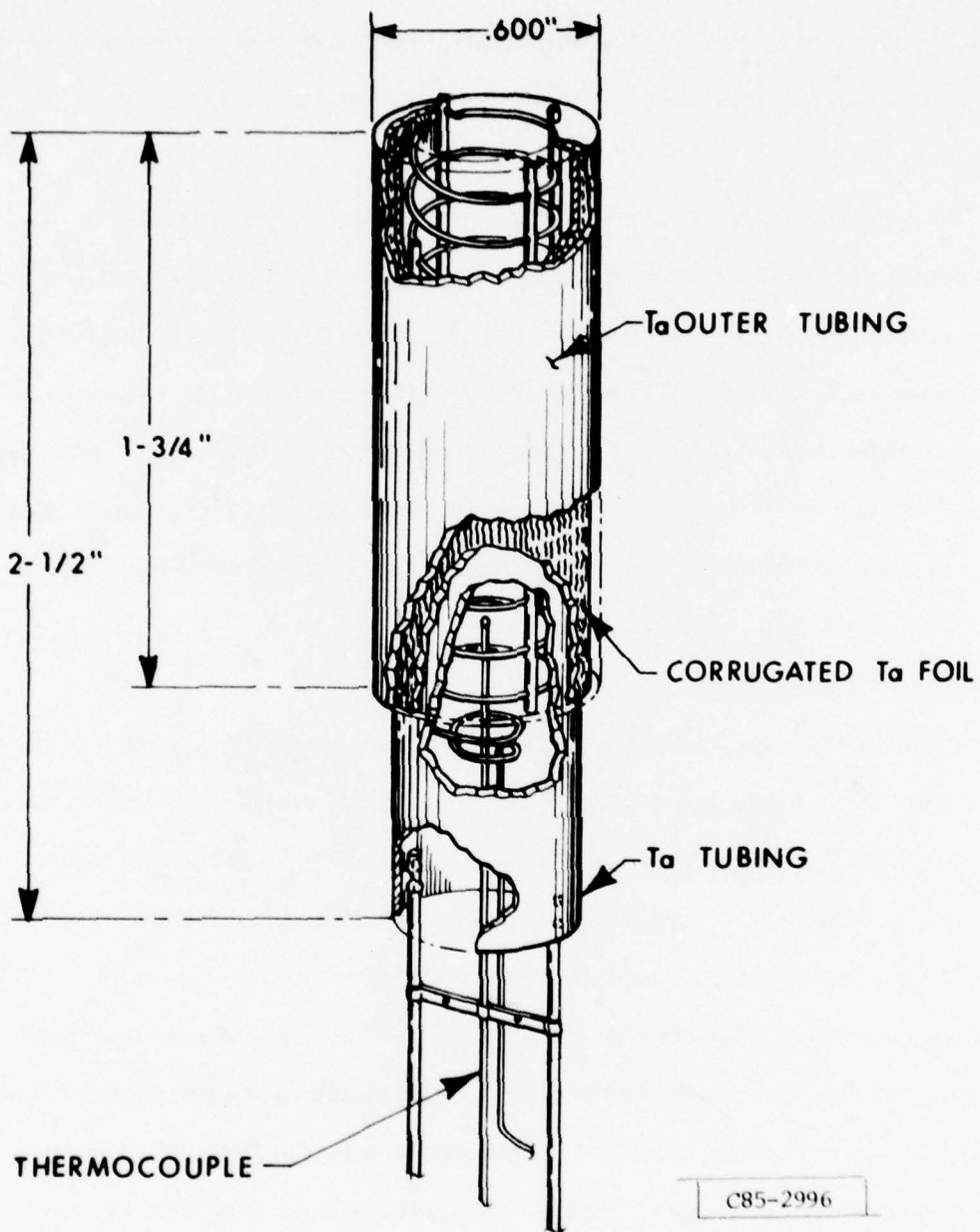


Fig. 3. Artist's view of MBE source heater assembly.

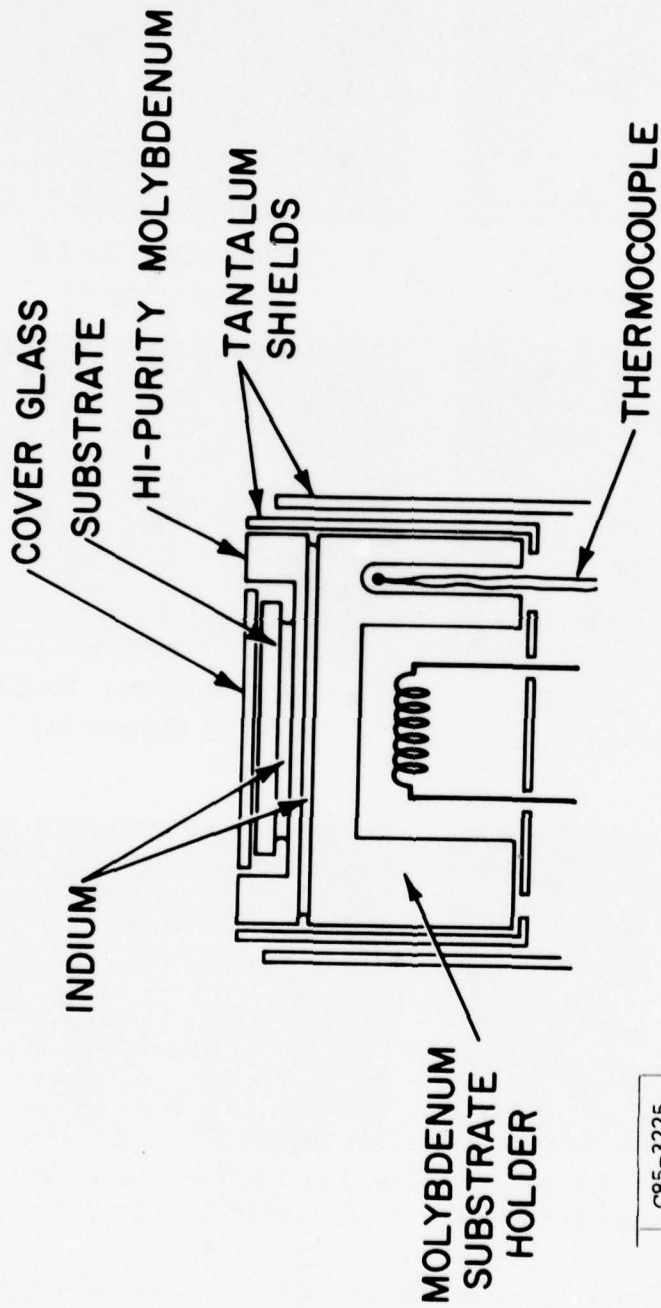
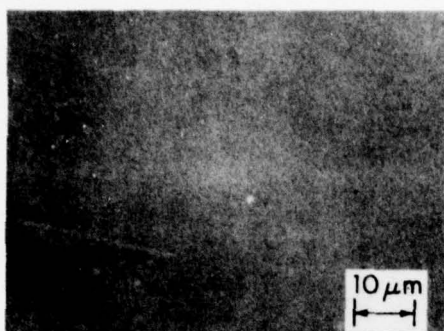
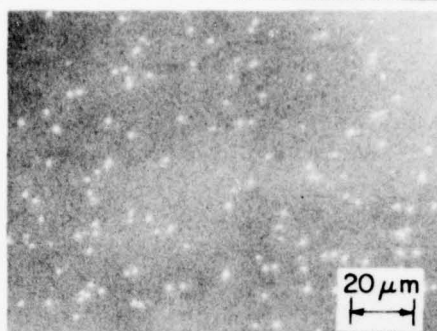


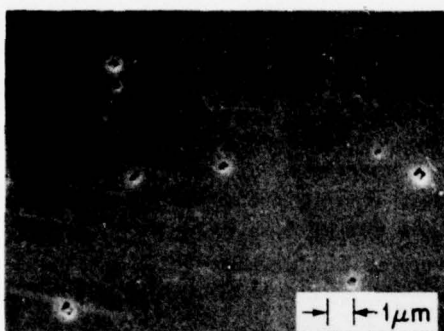
Fig. 4. Cross-sectional sketch of MBE substrate holder assembly.



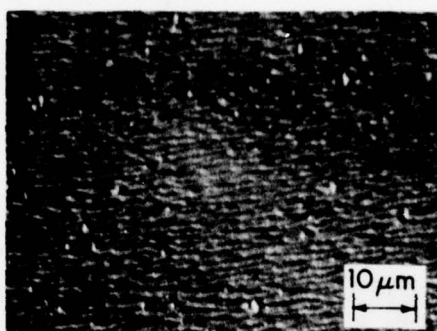
(a) CHEMICALLY ETCHED
($<0.5\text{-}\mu\text{m}$ damage)



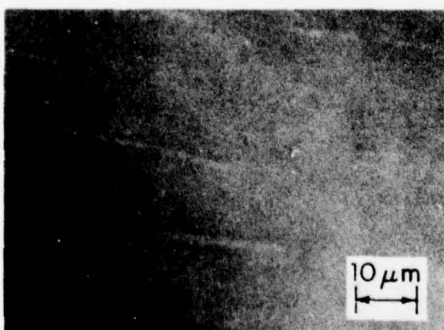
(b) THERMALLY ETCHED
(pits $\approx 10^5/\text{cm}^2$)



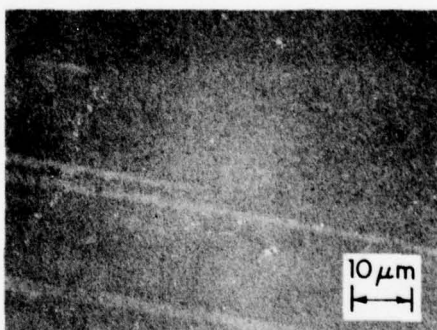
(c) THERMALLY ETCHED
(pits $\approx 10^5/\text{cm}^2$)



(d) EPI-LAYER $2\text{-}\mu\text{m}$ THICK
(570°C , $0.8\mu\text{m}/\text{hr}$)



(e) CHEMICALLY ETCHED
(thermally etched clean surface)



(f) EPI-LAYER $2\text{-}\mu\text{m}$ THICK
(570°C , $0.8\mu\text{m}/\text{hr}$)

Fig. 5. Microphotographs showing the effects of substrate surface damages on the MBE growth of GaAs.

Considerable effort has been put into correlating MBE film surface morphology with substrate orientation and quality and with the experimental growth parameters.⁴⁰ It is generally accepted that various dislocation lines appearing in the film can be attributed to a strained substrate or lattice mismatch. Dendritic growth usually results from faulty epitaxial conditions, and the pyramids or mounds which were observed on some of our early epitaxial layers result from some form of surface damage or contamination.

Using white light focused onto the substrate surface during growth, it was possible to observe the pyramidal growth as light scattering centers, usually after about 30 minutes of growing time. Using the same procedure with the substrate at the growth temperature and only the arsenic beam on the surface to prevent surface decomposition, similar light scattering centers were observed. Microscopic examination of these surfaces showed the scattering centers to be thermally etched pits resulting from a damaged surface. These pits became nucleation centers where the Ga and As were tightly bound, resulting in a very low surface mobility of the atoms. Small crystallites were formed, frequently misoriented with the substrate which resulted in the observed pyramids or mounds. Continued epitaxial growth on a surface with a high density of these defects would result in an overall roughness of the layer. This effect is illustrated in the interference contrast micro-photographs shown in Fig. 5. The smooth featureless surface shown in Fig. 5(a) was produced by a chemi-mechanical polish followed by a short chemical free-etch which removed 10 μm . From subsequent investigations it is estimated that this sample contains a small amount ($<2 \mu\text{m}$) of buried surface damage. This damage, shown in Fig. 5(b), is revealed by thermally etching the sample on a carbon heater strip in a H_2 atmosphere at 600°C for 15 minutes.

These conditions simulate the thermal etching which occurs in the MBE system. For this substrate, the pits formed by preferential evaporation from damaged areas have a density of $\approx 10^5/\text{cm}^2$. Figure 5(c) is a scanning electron micrograph of the pits showing the $\langle 100 \rangle$ surface symmetry. Figure 5(d) is an interference contrast micrograph of the surface of a $2\ \mu\text{m}$ -thick film grown on part of the substrate shown in 5(a). The surface irregularities do not occur only where the pits are formed, but over the entire surface. By contrast, Fig. 5(e) is a photograph of a thermally etched substrate prepared identically to that of 5(b) with the exception that several additional microns of material were removed in the final chemical free-etch. Most of the surface damage has been removed as evidenced by the comparatively low etch pit density. The surface topography of a $2\ \mu\text{m}$ -thick MBE layer grown on this surface is shown in Fig. 5(f). It is smooth and featureless.

The disadvantage of excessive chemical free-etching is that of rounding of the sample surface, an effect which can be detrimental when devices are fabricated using precise photolithographic techniques.

The current method of preparing GaAs substrates for MBE growth is a modification of a procedure developed at this Laboratory for vapor epitaxial growth. The wafers are string-saw cut 2° off from the (100) plane in the $\langle 211 \rangle$ direction. They are ground and chemi-mechanically polished on a polyurethane felt pad with a solution of 40 gm Na_2CO_3 in one liter of 1:1 H_2O and clorox. The polish removes 0.1 mm of material. The wafers are stored in this condition. Prior to mounting into the system the wafers are soaked in a KOH solution to remove any trace of mounting waxes, followed by a HCl soak to remove oxides. This procedure assures uniform etching in the subsequent step in which the sample is etched for 10 minutes in a 5:1:1 solution of H_2SO_4 , H_2O_2 and H_2O at 300 K. This final etch removes about $10\ \mu\text{m}$. The sample is then rinsed in high

purity water and blown dry with filtered nitrogen. Prior to each epitaxial growth run, the substrate surfaces were examined with an Auger cylindrical mirror analyzer operated at an electron beam voltage of 6 KV, a beam current of 275 μ A, and an Auger electron energy scan range of 0 to 2000 eV. The differential Auger spectrum of a chemically etched GaAs substrate prepared in the above manner is shown in Fig. 6(a). In addition to the Ga and As spectra, peaks corresponding to the characteristic energies of oxygen, carbon and sulfur are also seen. Figure 6(b) shows the spectrum of the same sample after heating for one minute at 600°C. The oxygen is completely gone. Finally, after ion sputtering the surface with a 10 mA, 500 eV argon ion beam for five minutes, all traces of the surface contamination have been removed. The peak attributed to sulfur is not always seen. Its origin is not known. Oxygen and carbon are introduced in the final etching and rinsing steps. By carefully quenching the final etch with CO₂-free water prior to exposure to air, it is possible to reduce the carbon contamination to a level where epitaxial growth is not affected. Thus a properly prepared GaAs surface requires only a slight thermal etch to remove the oxygen, prior to epitaxial growth.

C. Electron Diffraction Studies:

Figure 7 shows how Reflection Electron Diffraction⁴¹ (RED) is used as a guide in the growth of high-quality films. Three types of diffraction pattern are normally seen on the phosphor screen. A spot pattern is that obtained by transmission of electrons through a thin crystal, in this case the asperities of a rough surface. The Debye-Scherrer rings are typical of transmission through an amorphous or small grain polycrystal. The Kikuchi lines are observed where the surface has become so smooth that transmission through asperities is no longer possible and only two

C85-2989

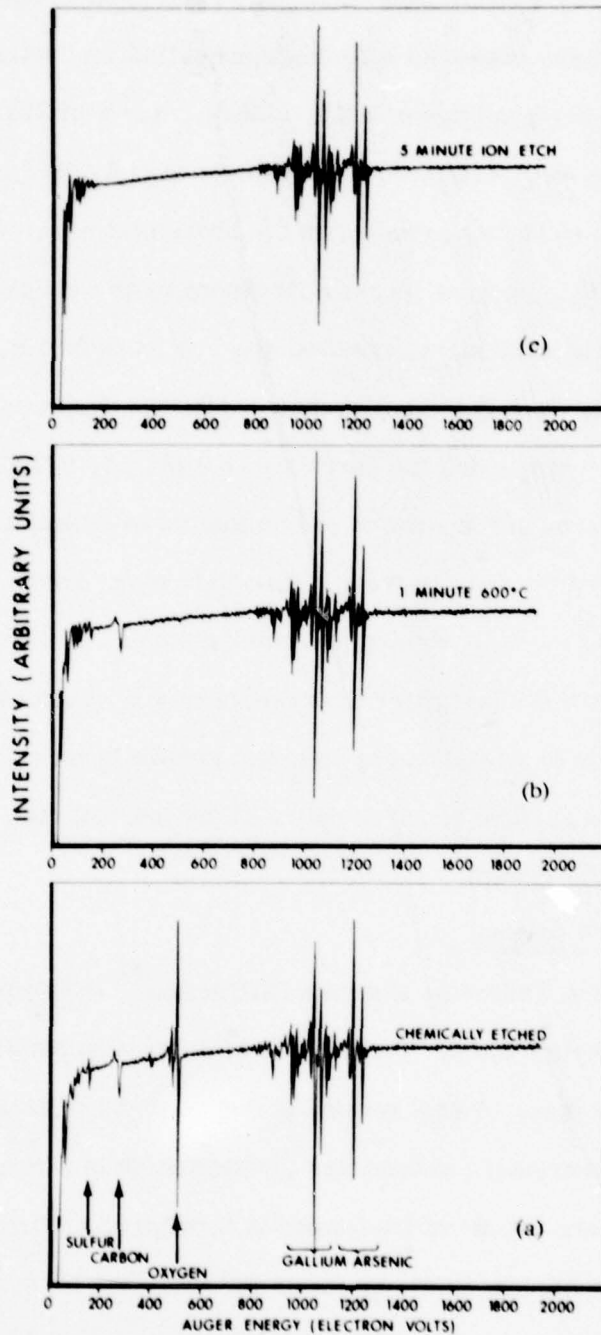


Fig. 6. Auger spectra of a GaAs substrate: (a) after chemically etching, (b) after thermal etching for 1 minute at 600°C, (c) after argon ion beam etching for 5 minutes.

C85-2988

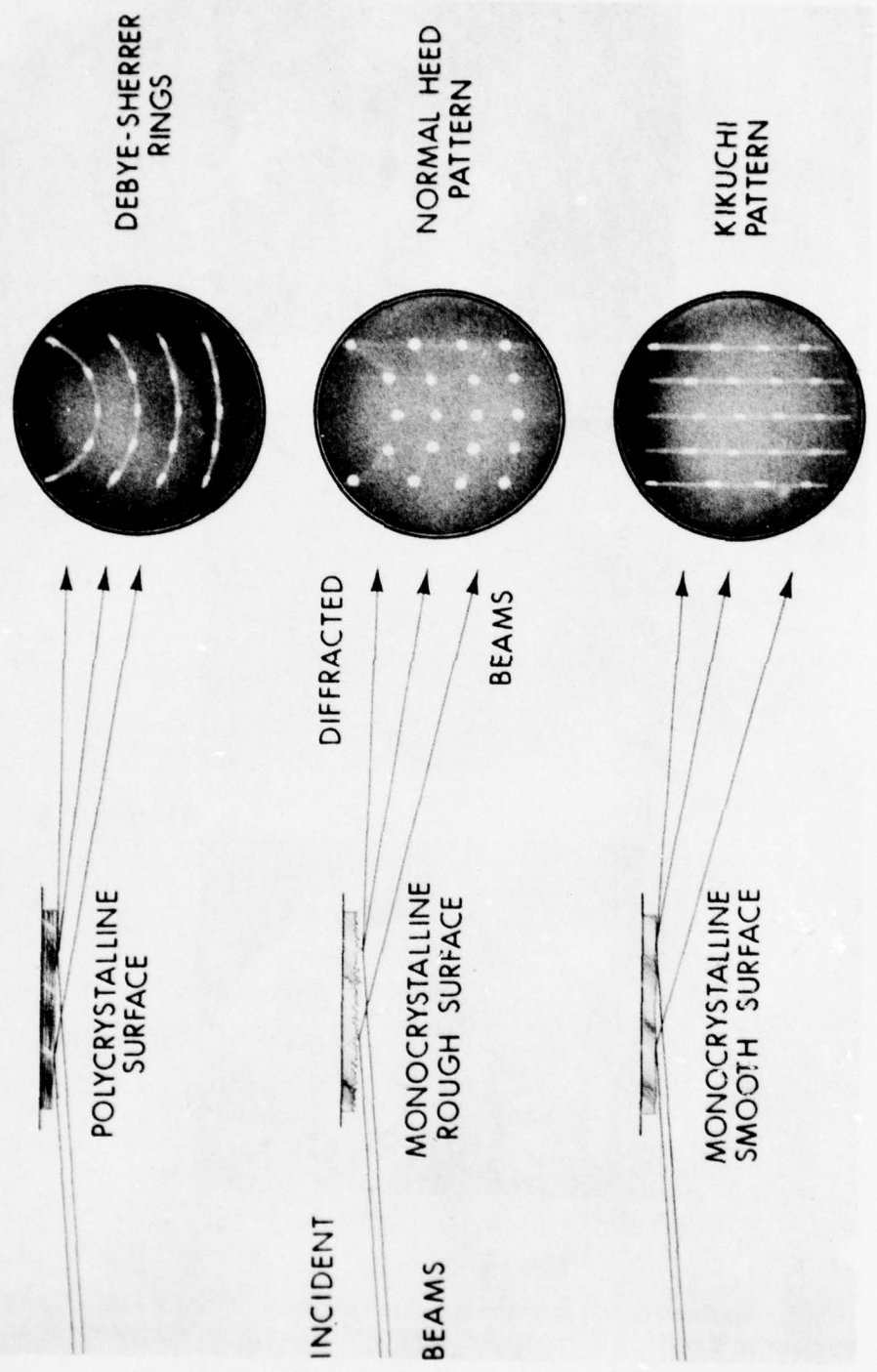
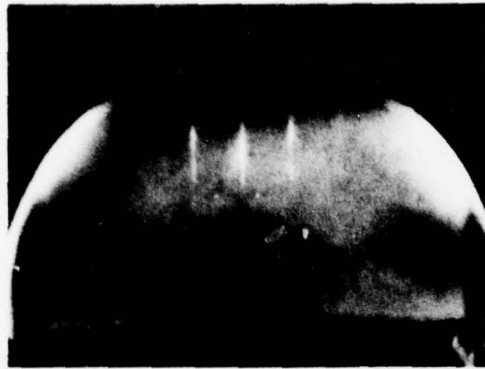
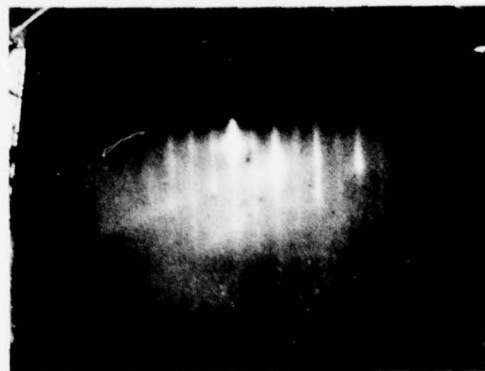


Fig. 7. Electron beam reflection electron diffraction patterns obtained from different substrate surfaces.

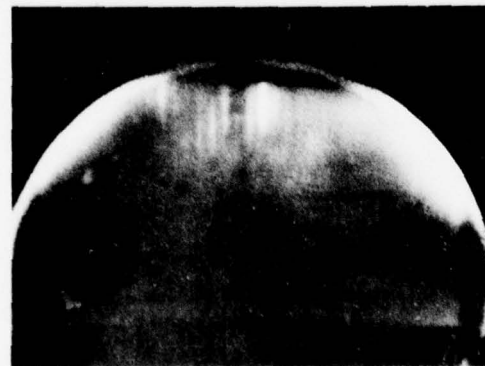
C85-3224



a



b



c

Fig. 8. Reflection electron diffraction patterns from a (100) GaAs surface in the [100] azimuth for (a) a stoichiometric surface, (b) an arsenic-rich surface and (c) a gallium rich surface.

dimensional diffraction is observed. An accurate quantitative structure analysis of the growing surfaces through observation of RED patterns is not feasible for several reasons. Because the angle between the incident and diffracted electron beams is small, it can be shown that the interplanar atomic spacings are related to the RED rings or spots by the expression;

$$d_i = \frac{\lambda L}{R_i}$$

where λ is the electron de Broglie wavelength, L is the distance between the sample and screen and R_i are the radii of the circular patterns defined by the RED rings or spots. Unfortunately L is not well defined because the electron beam at grazing incidence is spread over a large area of the sample and its precise position is not known. Also, precise azimuthal orientation of the sample is impractical since it would require a complex precision apparatus in the MBE system which would not interfere with the growth nor contribute to the contamination of the epitaxial layers. Even with these restrictions, however, the RED patterns provide valuable information about the growing surface layer.

Figure 8 shows high energy RED patterns (18 KeV electrons with the incident beam along the [110] azimuth) from a (100) GaAs surface. The initial diffraction pattern consisting of well defined spots is obtained from a chemically and thermally etched GaAs substrate. After depositing 150 Å of GaAs, the surface has become elongated in the direction normal to the surface. At the same time, additional features have appeared half way between the original columns of diffraction spots. These "1/2-order" streaks⁴² are due to a re-ordering of the surface atoms in such a manner that a dynamic equilibrium is established between the molecular species

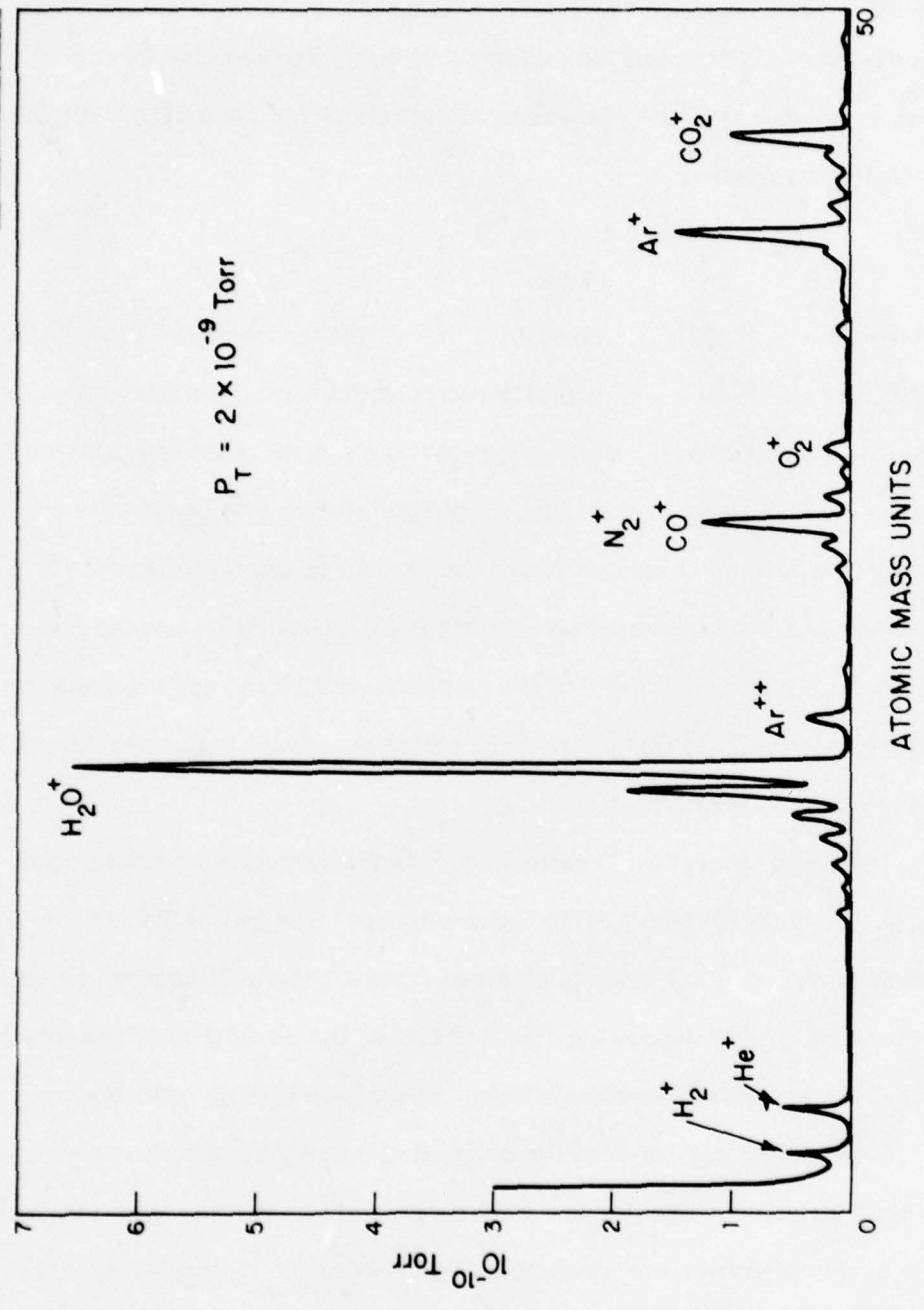


Fig. 9. Quadrupole mass analyzer spectrum of residual gases in the MBE growth chamber 16 hours after pumpdown.

in the vapor and that on the surface. For a given orientation, there are three patterns normally seen; that corresponding to a stoichiometric surface, a surface deficient of gallium or a surface deficient of arsenic. Figure 8(a) is the diffraction pattern in the [110] azimuth of a (100) stoichiometric surface which is seen prior to epitaxial growth. By adjusting the ratio As/Ga in the incident flux and the substrate temperature (which determines the decomposition rate of the substrate), the growth conditions can be set where the diffraction pattern of Fig. 8(a) is seen throughout the epitaxial growth. Figure 8(b) shows the diffraction pattern obtained under arsenic rich conditions and Fig. 8(c) is that seen for a gallium rich surface. Preliminary studies of the quality of MBE grown films as a function of the deviation from stoichiometry indicate that the highest quality films are those grown closest to stoichiometric conditions. More research is needed in this area and RED will undoubtedly be an important diagnostic tool for this study and for reproducibly obtaining optimum MBE growth conditions.

D. Mass Spectrum Analysis:

A UTI 300c quadrupole mass analyzer is used to monitor both residual gases and molecular fluxes incident on the substrate surface prior to and during epitaxial growth. All of the residual gases in our MBE growth chamber have relatively small masses and are seen in the range of 0 to 50 atomic mass units (amu). Larger mass hydrocarbons are only seen when the system is extensively dismantled for making repairs or modifications. These large mass hydrocarbons are easily removed by baking the entire system at 250°C for 24 hours. Figure 9 is a spectrum in the 0 to 50 amu range of the residual gases seen in the MBE growth chamber after changing substrates and overnight (16 hours) pumping. The system pressure is typically

C85-3137

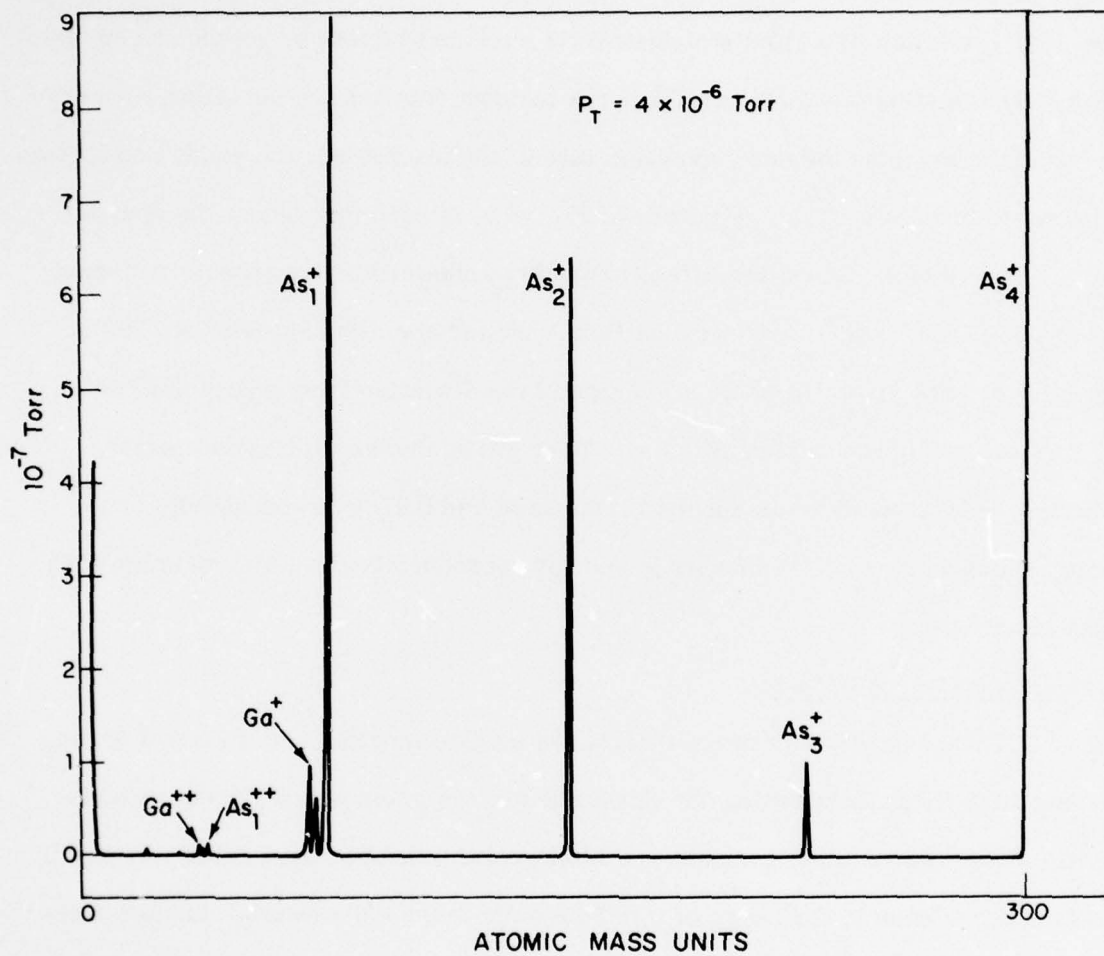


Fig. 10. Typical mass spectrum of molecular beams during the epitaxial growth of GaAs.

2×10^{-9} Torr. The spectrum is calibrated to give the partial pressures of the gases. The dominant species are labeled. The unlabeled peaks are either cracking patterns of the labeled peaks or low mass hydrocarbons. Some of the effects that residual gases have on MBE growth of GaAs are discussed in a later section. Figure 10 is a spectrum in the 0 - 300 amu range of the partial pressures of the incident molecular beam fluxes of arsenic and gallium and their cracking patterns taken during MBE growth of a GaAs layer. The arsenic source used in this growth was 6-9's pure crystalline arsenic. The calculated As_4/Ga ratio is approximately 10:1. With the substrate temperature at $575^{\circ}C$, the GaAs epitaxial layer is grown on the arsenic-rich side of the GaAs solidus field.

E. Epitaxial Growth Parameters:

The MBE growth rate as a function of gallium source temperature is plotted in Fig. 11. The experimental points were determined using thicknesses measured with a scanning electron microscope and scheduled growth times. The solid curve was calculated using the Knudsen equation for incident molecular flux density⁴³:

$$F = \frac{P(T)A}{4\pi L^2 \sqrt{2\pi m k T}}$$

where

$P(T)$ = equilibrium vapor pressure at temperature T

A = aperture area of source

L = distance from source to substrate

m = mass of evaporant species

For these experiments, the source control thermocouple is embedded between the furnace wall and the pyrolytic boron nitride crucible containing the Ga. This control thermocouple was calibrated by immersing a second thermocouple in the Ga liquid.

C85-3226

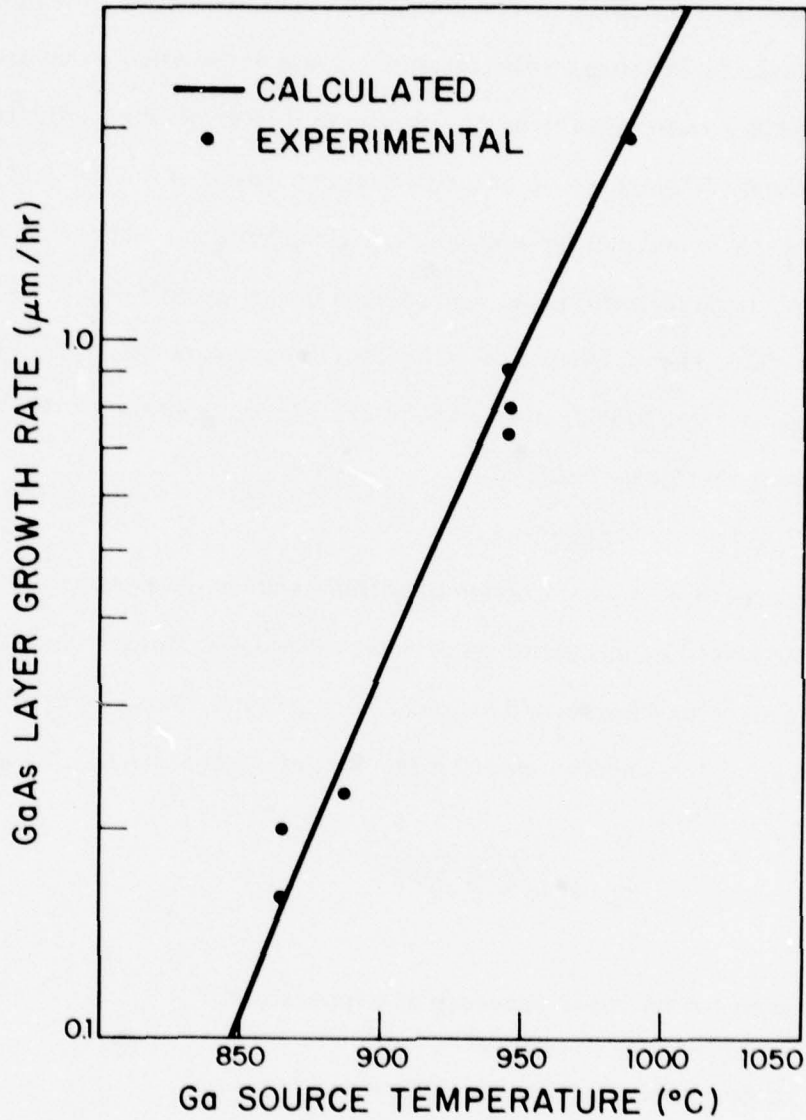


Fig. 11. Epitaxial growth rate of GaAs as a function of Ga effusion cell temperature.

The results indicate that films thicknesses can be controlled to within about 10% by simply controlling the Ga source furnace temperature.

For a given Ga flux, the required As flux is determined by the substrate temperature. Because the As sticking coefficient is unity⁴⁴ when the substrate surface is Ga-rich and approximately zero for a stoichiometric GaAs surface, the epitaxial layer does grow near stoichiometric in an excess arsenic environment. Most layers were grown at a rate of 3 Å/sec, a substrate temperature of 575°C and an As₄/Ga ratio of 5.

F. Electrical Properties:

Carrier concentrations and mobilities obtained from van der Pauw and resistivity measurements on some early films are shown in Table II. The thicknesses of these films ranged from 2 μm to 5 μm. The data clearly show that the unintentionally doped films are p-type and have nearly two orders of magnitude variation in carrier concentration. The Si-doped films are n-type with concentrations varying monotonically for Si source temperatures above 850°C. With Si-source temperatures below 850°C the free carrier concentration varies randomly. This probably reflects the degree of compensation resulting from system background impurities which invariably differ from run to run. That the films are highly compensated is also reflected in the low mobility values, particularly at 77 K.⁴⁵ Corresponding 77 K mobilities for uncompensated n-type GaAs grown by vapor phase epitaxy (VPE)⁴⁵ are about an order of magnitude greater than those shown in Table II.

G. Effect of H₂ on Electrical Properties:

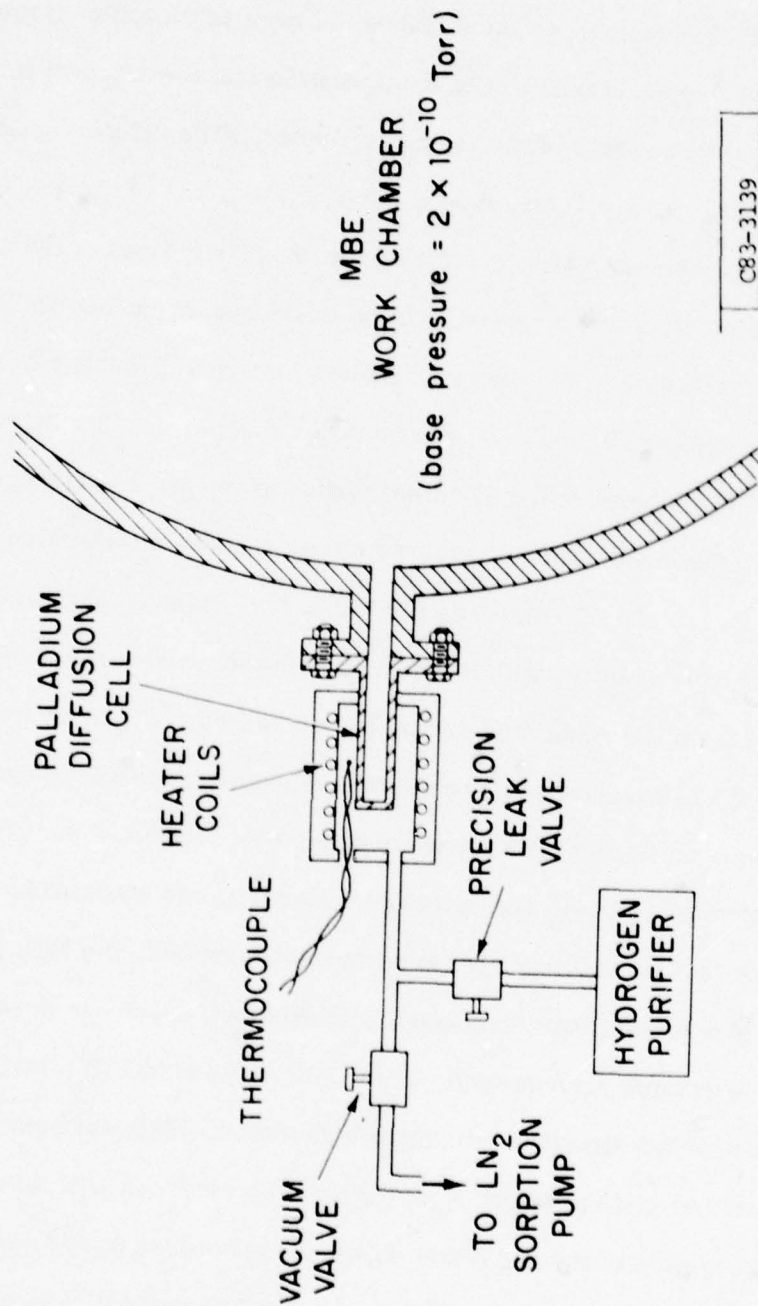
For a growth rate of 3 Å/sec the incident Ga flux density is 6×10^{14} atoms/cm² sec. Assuming that the observed 77 K mobilities listed in Table II are governed primarily by ionized impurity scattering, the films would contain 10^{17} cm⁻³ total impurities. To

TABLE II
 ELECTRICAL CHARACTERISTICS OF GaAs MBE FILMS GROWN IN ULTRA-HIGH VACUUM
 (Residual gas pressure $\approx 2 \times 10^{-10}$ Torr)

Sample No.	Dopant	Si-Source Temperature °C	Carrier Type	Free Carrier Concentration (cm ⁻³)		Free Carrier Mobility (cm ² /Vsec)	
				300 K	77 K	300 K	77 K
9B	undoped	-	p	4.0×10^{15}	4.8×10^{14}	226	278
10B	undoped	-	p	5.0×10^{13}	1.0×10^{10}	185	32
14A	Si	750	p	1.5×10^{16}	4.0×10^{15}	202	1187
21B	Si	750	p	3.6×10^{15}	1.7×10^{15}	295	1837
16A	Si	800	n	2.6×10^{14}	2.5×10^{14}	4804	3654
18A	Si	800	n	4.8×10^{15}	3.2×10^{15}	5122	7708
16B	Si	850	n	3.8×10^{15}	3.7×10^{15}	4276	5000
15A	Si	900	n	1.0×10^{16}	8.5×10^{15}	2783	3503
15B	Si	950	n	1.8×10^{17}	1.8×10^{17}	2609	2865
27B	Si	850	n	2.0×10^{16}	1.4×10^{16}	4609	5315
33B	Si	770	n	1.0×10^{15}	1.0×10^{15}	2272	5423

obtain this impurity level with unity sticking coefficient, the residual impurity flux density would be 10^9 molecules/cm² sec. Since the limit of detection of the mass analyzer used is 10^{11} molecules/cm² sec it is possible that the residual impurity or impurities are not detectable in the vacuum chamber. The detected gaseous species, shown in Fig. 9, are H₂He, C_xH_y, H₂O, O₂, N₂, CO, Ar and CO₂ with their corresponding cracking patterns. Within the sensitivity limit of the analyzer no other foreign impurities are detected. Of the above gases, carbon and oxygen are potential dopants in GaAs. Carbon is a shallow acceptor⁴⁶ 0.026 eV above the valence band. Oxygen is believed to be a deep donor⁴⁷ about 0.63 eV below the conduction band. The incorporation of either carbon or oxygen into the epitaxial layer must involve the dissociation of one or more of the above molecules at the substrate temperature. The dissociation products, i. e., ionized atomic carbon or oxygen, are both highly reactive with hydrogen and in the presence of a hydrogen atmosphere could form the respective hydrogen compounds. All of the hydrogen compounds formed are gases at room temperature and are expected to have low sticking coefficients on GaAs at the growth temperature. It should be noted also that the above reactions with H₂ are reversible reactions and equilibrium is obtained.

To be certain that no additional gases were introduced into the MBE growth chamber when the hydrogen was introduced, a special technique was devised. This technique is demonstrated schematically in Fig. 12. The output of a palladium diffusion cell is attached directly to the ultra-high vacuum MBE work chamber. The palladium is heated to a temperature at which only the hydrogen will diffuse through. As long as the input side of the palladium diffusion cell is free of hydrogen or hydrogen compounds, the MBE work chamber can be pumped to its original base pressure of



C83-3139

Fig. 12. Diagram of method used to introduce pure hydrogen into MBE growth chamber.

2×10^{-10} Torr. This is easily achieved by evacuating the input of the cell to a pressure of 5 microns with an LN_2 sorption pump. A precision leak valve is then used to admit hydrogen into the input side of the palladium diffusion cell which then diffuses rapidly into the system.

Several GaAs epitaxial layers were grown in the presence of about 10^{-6} Torr of H_2 . The electrical properties of these films are shown in Table III. There are two significant differences in the properties of these films and those grown without the H_2 backfill shown in Table II. First, the mobilities both at 300 K and 77 K are considerably higher for the films grown in the presence of H_2 . Second, for the same silicon source temperature a higher net donor concentration is generally obtained for the films grown in the presence of H_2 . In fact, for a silicon source temperature of 750°C the films have been converted from p-type to n-type with the addition of H_2 under controlled experimental conditions. Both the higher mobilities and net increase in donor concentration could be explained by a reduction in carbon doping in the presence of H_2 . An exception to the doping change occurs in films 27 A and 27 B where the concentration is slightly higher when H_2 is not used. These films were grown after a new source furnace was put into the system and an unusually high background pressure of CO was present. This suggests that the hydrogen is also affecting the incorporation of oxygen and whether the free carrier concentration is increased or decreased when growing in a H_2 atmosphere may depend on the relative abundance of the different background gases. The effect of hydrogen on residual impurity compensation is graphically illustrated in Fig. 13. The net donor concentrations, $N_D - N_A$, were obtained from Hall measurements and the total ionized impurity concentrations, $N_E + N_A$, were obtained from the 77 K mobility analysis.⁴⁵ It is clear that substantial reductions in $N_D + N_A$ have been achieved. As shown in Fig. 13,

TABLE III
ELECTRICAL CHARACTERISTICS OF GaAs MBE FILMS GROWN
IN THE PRESENCE OF 10^{-6} Torr H_2

Sample No.	Dopant	Si-Source Temperature °C	Carrier Type	Free Carrier Concentration (cm^{-3})		Free Carrier Mobility ($cm^2/Vsec$)	
				300 K	77 K	300 K	77 K
19A	Si	800	n	6.5×10^{15}	6.0×10^{15}	6700	18600
19B	Si	800	n	4.5×10^{15}	3.5×10^{15}	6100	13800
20A	undoped	-	p	2.0×10^{15}	3.0×10^{14}	390	4900
20B	Si	775	n	2.7×10^{15}	2.5×10^{15}	7000	25100
22A	Si	750	n	2.0×10^{15}	2.2×10^{15}	7200	28100
27A	Si	850	n	7.9×10^{15}	7.0×10^{15}	6000	12600
29A	Si	750	n	2.9×10^{15}	2.6×10^{15}	6020	16200
32A	Si	775	n	4.0×10^{15}	4.0×10^{15}	6300	18400
33A	Si	770	n	5.0×10^{15}	4.0×10^{15}	6300	16800
36B	Si	900	n	1.0×10^{16}	1.0×10^{16}	6300	18500
37A	Si	1000	n	2.8×10^{16}	2.2×10^{16}	5900	10800
37B	Si	950	n	1.1×10^{16}	9.0×10^{15}	6600	16900
39A	Si	775	n	1.2×10^{15}	1.1×10^{15}	6500	37200
39B	Si	780	n	1.4×10^{15}	1.2×10^{15}	6600	23700
40A	Si	775	n	2.3×10^{15}	2.2×10^{15}	6000	20700

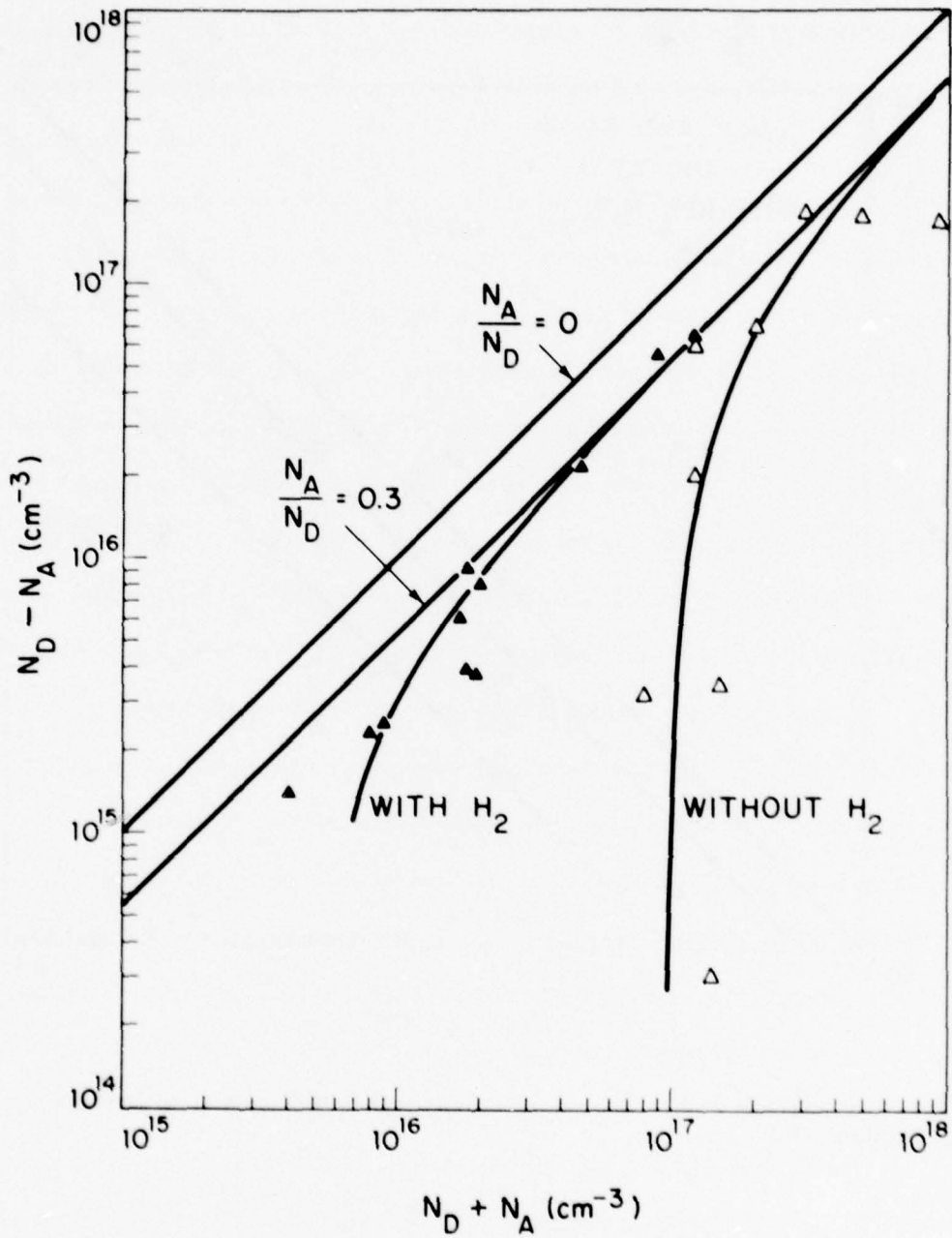


Fig. 13. Net donor concentration ($N_D - N_A$) as a function of total ionized impurity concentration ($N_D + N_A$) at 77 K with and without hydrogen. Lines $N_A/N_D = 0$ and $N_A/N_D = 0.3$ are drawn for reference.

C85-3142

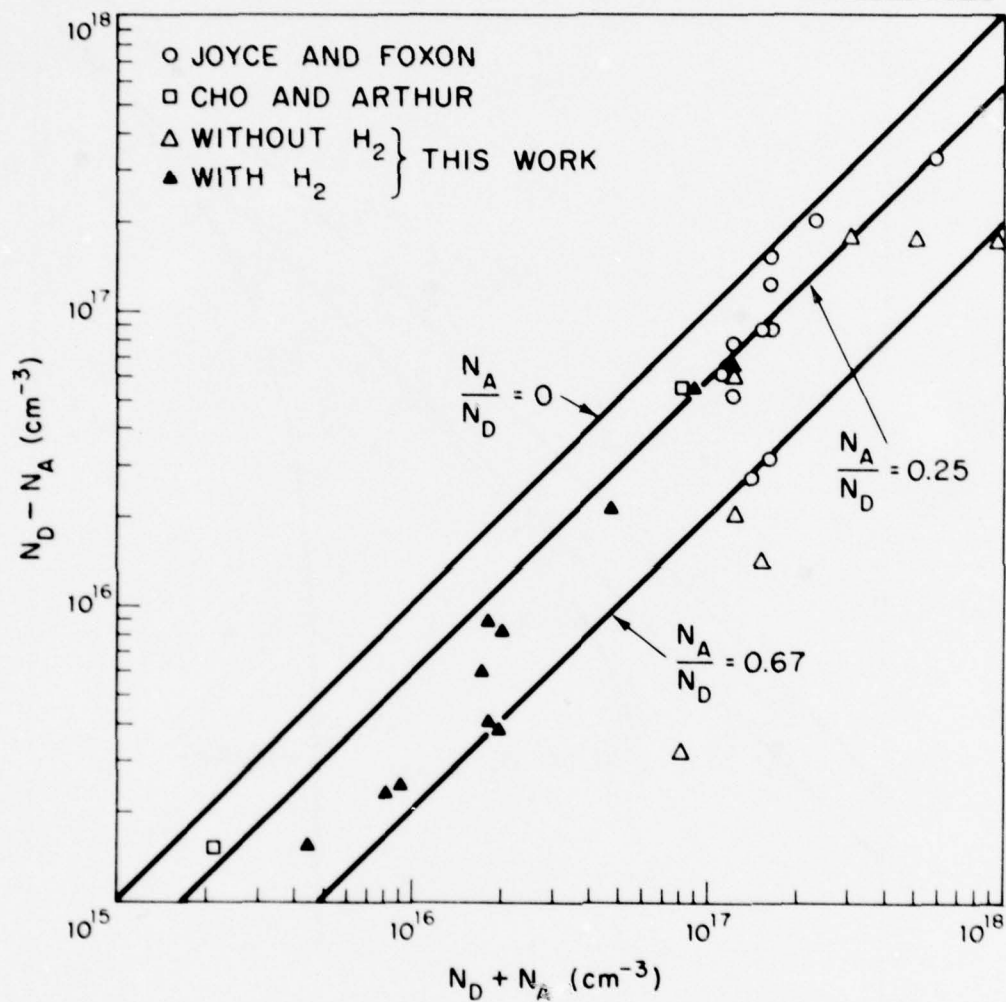


Fig. 14. Comparison of $(N_D - N_A)$ vs $(N_D + N_A)$ in this report with other published data.

a 50 times reduction was attained for the films with the lowest net donor concentrations. There is very little 77 K mobility data available on MBE grown n-type GaAs layers with which our results can be compared. All of the published data are plotted in Fig. 14 with our current results. The highest purity sample reported to date was that obtained by Cho and Arthur¹ with a total ionized impurity concentration of $2.1 \times 10^{15} \text{ cm}^{-3}$ and a 77 K mobility of $50,000 \text{ cm}^2/\text{Vsec}$. This value has apparently never been reproduced. All of the remaining data is for samples with $N_D + N_A \gtrsim 10^{17} \text{ cm}^{-3}$ which corresponds to our limiting values without the use of H_2 .

H. Photoluminescence Measurements:

The photoluminescence properties of these samples were also examined to gain more information on the effect of hydrogen introduced during growth. Two optical systems were used for these measurements. To investigate the broad band deep level luminescence frequently seen in GaAs,⁴⁸ the samples were pumped with a 500 mW krypton laser. The luminescence was observed with a CsBr prism spectrometer and synchronously detected with a cooled PbS detector. For band edge luminescence measurements a 50 mW HeNe laser was used. The edge luminescence was dispersed with a 3/4 meter grating spectrometer and synchronously detected with a cooled photomultiplier equipped with a GaAs photocathode.

Results of the deep level photoluminescence measurements made at 80 K on two n-type silicon-doped films and on two p-type undoped films with different hydrogen pressures are shown in Figs. 15 and 16, respectively. The electrical characteristics of each film are shown in the insets. The dominant effects of the hydrogen in each case are the large reduction in intensity of deep-level luminescence and an increase in band-edge luminescence. The deep level luminescence with maxima at 0.88 eV in the

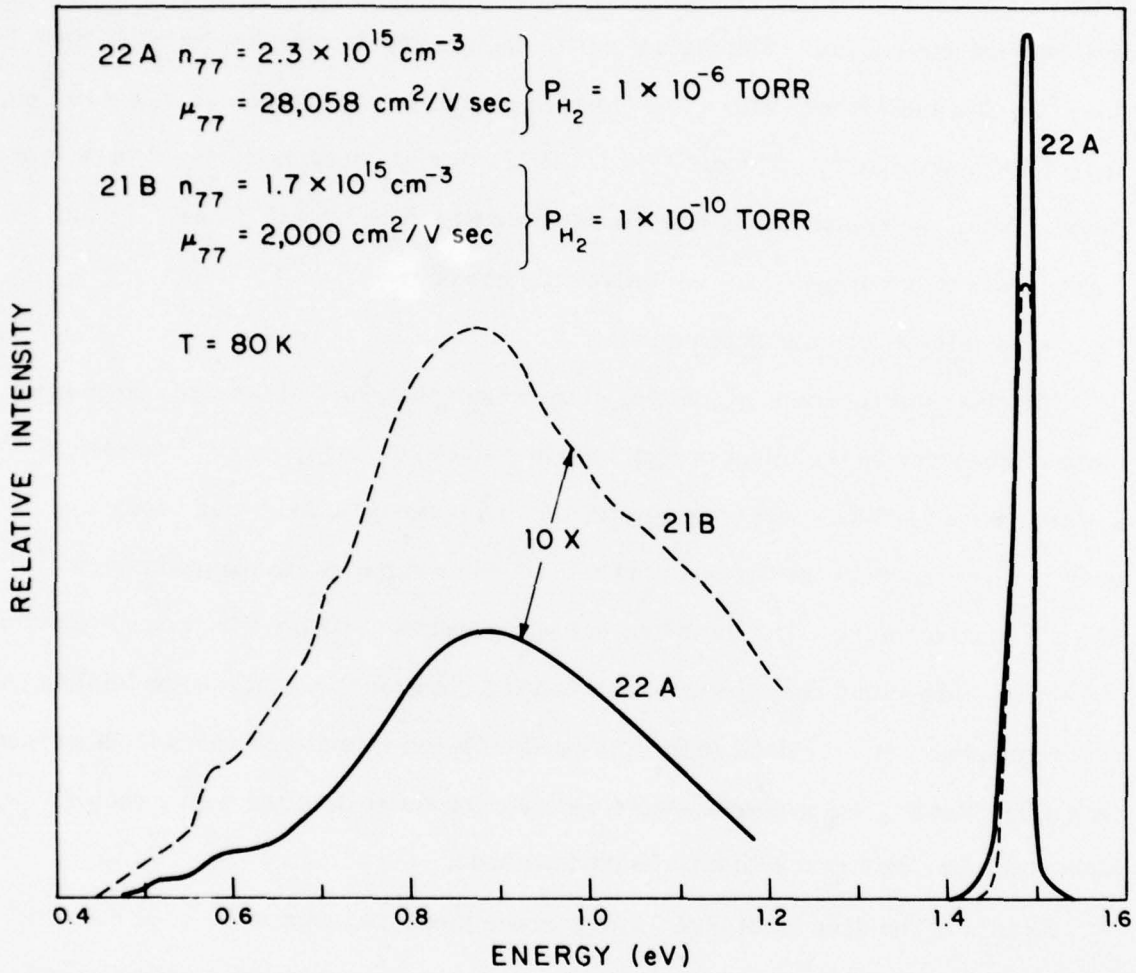


Fig. 15. Effect of H_2 ambient pressure on the band-edge (1.49 eV) and deep level (0.88 eV) photoluminescence in n-GaAs MBE films.

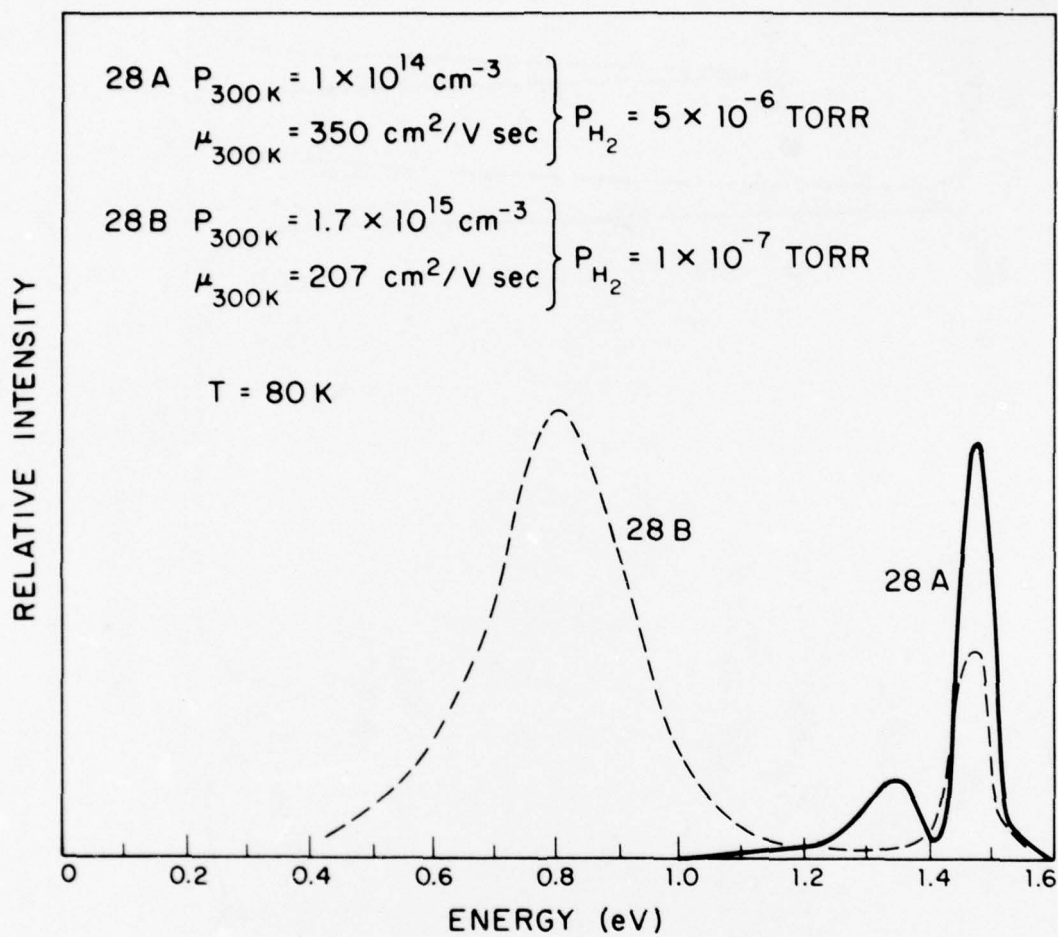


Fig. 16. Effect of H_2 ambient pressure on the band-edge (1.49 eV) and deep level (0.80 eV) photoluminescence in p-GaAs MBE films.

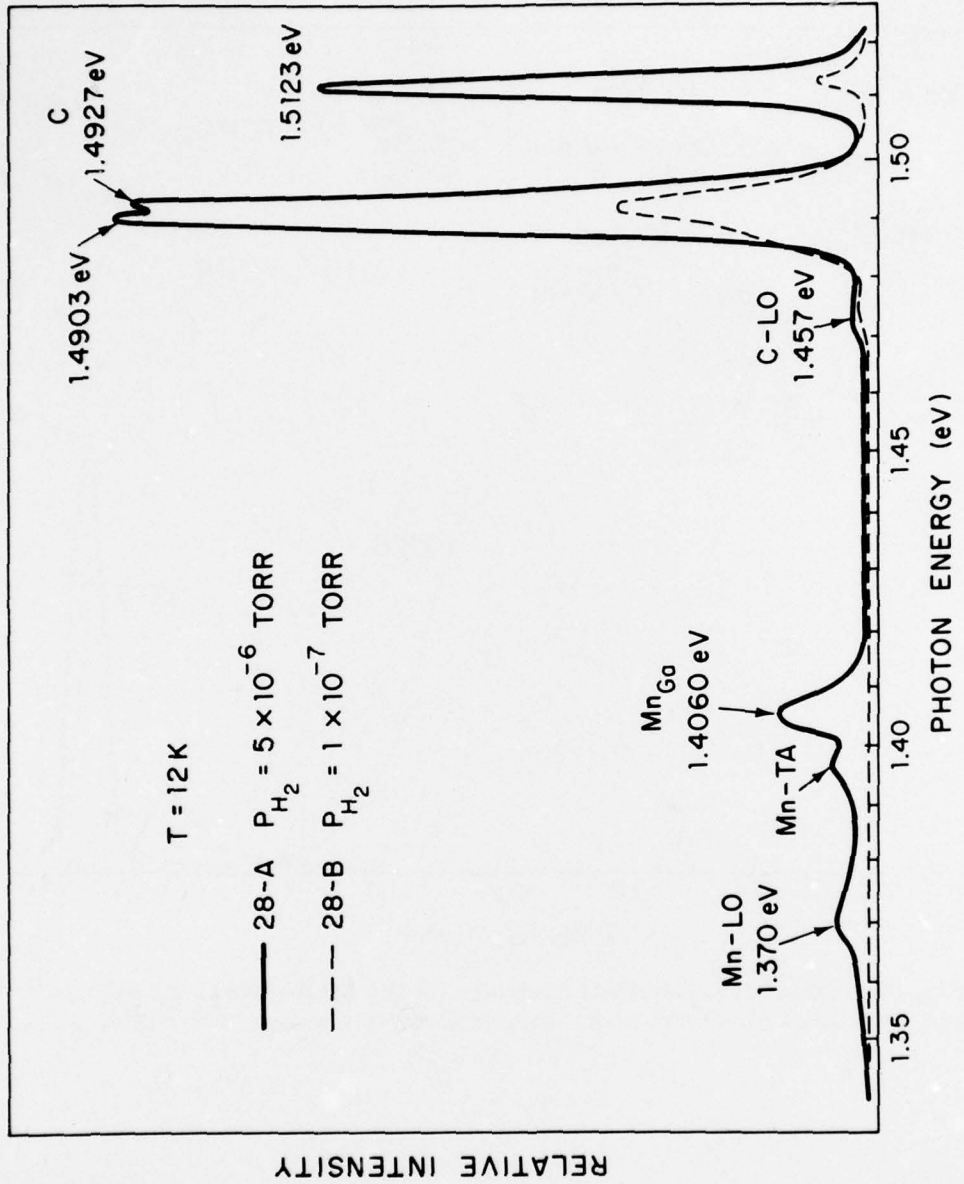


Fig. 17. Detail of band-edge photoluminescence spectra at 12 K for the same p-type GaAs MBE films as for Fig. 16.

n-type films and at 0.80 eV in the p-type sample are believed due to oxygen or oxygen complexes.⁴⁸

The band-edge luminescence spectra for samples 28 A and 28 B were examined more closely at 10 K and are shown in Fig. 17. The peak at 1.512 eV is attributed to neutral acceptor bound-exciton transitions and the double peaks at 1.4927 eV and 1.4903 eV are believed to be due to free-electron to carbon acceptor and donor-to-carbon acceptor pair transitions, respectively.^{49,50} Although this doublet is not always seen, the relative intensity of the 1.512 eV peak always increases relative to the carbon acceptor transitions when excess hydrogen is added during growth. This result suggests that the number of carbon acceptors is reduced when H₂ is present. The peak at 1.4060 eV is attributed to Mn on a Ga site.⁵¹ Phonon replica are also observed.

I. Growth of In_{1-x}Ga_xAs on InP

The ultimate goal of the contract is to grow MBE films of In_{1-x}Ga_xAs_{1-y}P_y on InP and to evaluate the performance of devices made with these films. However, phosphorus is an extremely volatile element and once introduced into the MBE system traces of phosphorus will always be present unless elaborate cleaning procedures are employed to remove it. In view of this it seems judicious to first investigate the properties of the ternary compound, In_{1-x}Ga_xAs, as grown on an InP substrate. The InP substrate preparation procedures will likely be the same in both systems as will the control of the In and Ga fluxes in the incident molecular beams. The ternary compound is also of interest in that the 300 K mobilities are found to increase monotonically from 7000 cm²/Vsec for GaAs²³ to 16700 cm²/Vsec for InAs.²⁴

To determine feasibility, two attempts were made to grow In_{1-x}Ga_xAs on InP using different In/Ga flux ratios and a substrate temperature of 500°C. The In and

Ga fluxes were set for a growth rate of about 3 Å/sec. The As/In_{1-x}Ga_x ratio was 10. Both films were crystalline with x = 0.22 and x = 0.37. In both cases an excess of In and Ga was observed on the surfaces, indicating the need for a higher As/In_{1-x}Ga_x ratio with the substrate temperature at 500°C. These results are encouraging and indicate it should be straightforward to grow In_{0.53}Ga_{0.47}As, which lattice matches InP, on an InP substrate.

If the indium and gallium molecular beams are derived from separate sources, the relative position of the sources with respect to the substrate can result in a significant variation in the composition of the grown film, particularly for large area films. If a specific In/Ga ratio is required, this problem can be circumvented by mixing the In and Ga in the same source. The partial pressures of the indium and gallium from such an alloy are given by:

$$P_{\text{In}} = P_{\text{In}}^{\circ} \gamma_{\text{In}} \chi_{\text{In}}$$

$$P_{\text{Ga}} = P_{\text{Ga}}^{\circ} \gamma_{\text{Ga}} \chi_{\text{Ga}}$$

where,

P_{In}° and P_{Ga}° are the equilibrium vapor pressures of elemental In and Ga at the alloy temperature, χ_{In} and χ_{Ga} are the mole fractions of In and Ga and γ_{In} and γ_{Ga} are the activity coefficients of In in Ga and of Ga in In, respectively. The thermodynamic expressions for the activity coefficients are:

$$RT \ln \gamma_{\text{In}} = \alpha_{\text{In Ga}}^{\ell} \chi_{\text{Ga}}^2$$

$$RT \ln \gamma_{\text{Ga}} = \alpha_{\text{In Ga}}^{\ell} \chi_{\text{In}}^2$$

where $\alpha_{\text{In Ga}}^{\ell}$ is the interaction energy of In and Ga in the liquid phase. For Ga-In melts, two values of interaction energy, $\alpha_{\text{In Ga}}^{\ell} = 1060$ cal/mole (Panish & Rlegems)⁵² and $\alpha_{\text{In Ga}}^{\ell} = 1850$ cal/mole (Pearsall & Hapson)⁵³ are available. Because the above expressions for γ are logarithmic, the difference in these values of $\alpha_{\text{In Ga}}^{\ell}$ results in a relatively insignificant change in vapor pressures for In and Ga at least for $x_{\text{Ga}} \approx x_{\text{In}} \times 0.5$. With these considerations, it should be possible to grow uniform homogeneous epitaxial films of $\text{In}_{1-x}\text{Ga}_x\text{As}$ on InP, while maintaining a precise In/Ga ratio.

Extending this concept to the growth of $\text{In}_{1-x}\text{Ga}_x\text{As}_{1-y}\text{P}_y$ on InP, a similar procedure could be considered using a ternary alloy of Ga-As-P for the control of the As/P ratio. The vapor pressure of phosphorus, however, is three orders of magnitude larger than that of arsenic; therefore the mole fraction of phosphorus required would be small and a large amount of the melt is needed if several epitaxial layers are to be grown between source changes. An alternative procedure which is being introduced into our MBE system is to mix gases such as AsH_3 and PH_3 in the desired ratio outside of the system and introduce the mixture into the system through a precision leak valve. It is expected that these gases will decompose at the substrate surface to supply the desired arsenic and phosphorus. The resulting hydrogen present should be beneficial to the growth of high quality epitaxial layers.

III. SUMMARY

The research performed in the first year of this contract has led to a significant advancement in the state-of-the-art of the MBE growth of GaAs and to new insights in MBE technology for the growth of other compounds as well. The introduction of H_2 into the MBE growth chamber during the growth of GaAs layers has significantly increased the carrier mobility in these films. Strong evidence is shown that the effect of the H_2 is to reduce the incorporation of residual impurities such as carbon and oxygen which are likely to be derived from the system residual gases even though these gas pressures are in the range of 10^{-10} Torr or less. The significance of this discovery may be far reaching for the growth of the quaternary compounds of GaInAsP in that it allows the possible use of AsH_3 and PH_3 as sources of As and P. Not only can these gases be precisely mixed outside of the MBE system for the accurate control of the As/P ratio, but the decomposition which should occur at the substrate will result in an abundance of hydrogen ($H_2^+ + H_1^+$) which has been shown to significantly improve the electrical characteristics of the GaAs layers. It should be noted that the introduction of AsH_3 and PH_3 will in no way compromise the advantages of MBE growth. The partial pressures of these gases will be about 10^{-6} Torr where their mean-free-paths are several orders of magnitude larger than the substrate distance. Also, the growth of the quaternary films is controlled entirely by the In and Ga fluxes since the sticking coefficients of As and P are essentially zero unless In or Ga are present.

IV. REFERENCES

1. A. Y. Cho and J. E. Arthur, *Prog. in Solid State Chem.* 10 (1975).
2. A. Y. Cho, *J. Vac. Sci. Tech.* 8, 531 (1971).
3. A. Y. Cho and M. B. Panish, *J. Appl. Phys.* 43, 5118(1972).
4. L. L. Chang, L. Eoaki, W. E. Howard, R. Ludeke and G. Schul, *J. Vac. Sci. Tech.* 10, 655(1973).
5. M. Naganuma and K. Tabahashi, *Phys. Stat. Sol.*, (a) 31, 187(1975).
6. Nobutoshi Matsunaga, Mitsuru Naganuma and Kiyoshi Tabahashi, *Proc. 8th Int. Conf (1976) on Solid State Devices; Jap. J. Appl. Phys.* 16, Suppl 16-1, 443(1977).
7. B. A. Joyce and C. T. Foxon, *Proc. 8th Int. Conf. (1976) on Solid State Devices; Jap. J. Appl. Phys.* 16, Suppl 16-1, 17(1977).
8. M. Ilegems, *J. Appl. Phys.* 48, 1278(1977).
9. I. Hayashi, M. B. Panish and P. W. Foy, *Appl. Phys. Lett.* 17, 109(1970).
10. Zh. I. Alferov, V. M. Andreev, D. Z. Garbuzo, Yuv V. Zhilgaev, E. P. Morozov, E.L. Portnoi and V.G. Trofim, *Tekh. Poluprov* 4, 1826(1970).
11. P. R. Selway, A. R. Goodwin and C. M. Phillips, *4th Ann. Conf. Solid State Devices, Oxford (1970)*.
12. G. E. Stillman, C. M. Wolfe, A. G. Foyt and W. T. Lindley, *Appl. Phys. Lett.* 24, 8(1974).
13. R. G. Eden, *Proc. IEEE* 63, 32(1975).
14. J. S. Escher, G. A. Antypas and J. Edgecumbe, *Appl. Phys. Lett.* 29, 153(1976).
15. J. J. Coleman, N. Holonyak, M. J. Ludowise, P. D. Wright, W. O. Gronev and D. L. Kuene, *Appl. Phys. Lett.* 29, 167(1976).
16. P. D. Wright, J. J. Coleman, N. Holonyak, M. J. Ludowise and G. E. Stillman, *Appl. Phys. Lett.* 29, 18(1976).
17. J. J. Hsieh, J. A. Rossi and J. P. Donnelly, *Appl. Phys. Lett.* 28, 709(1976).

18. R. L. Moon, G. A. Antypas and L. W. James, *J. Electron. Mater.* 3, 635, (1974).
19. M. Horiguchi, *Electron. Lett.* 12, 311 (1976).
20. D. N. Payne and W. A. Gambling, *Electron. Lett.* 11, 176 (1975).
21. M. A. Littlejohn, J. R. Hauser and T. H. Glisson, *Appl. Phys. Lett.* 30, 242 (1977).
22. S. Baskaron and P. N. Robson, *Electron. Lett.* 8, 137 (1972).
23. A. R. Calawa, *Appl. Phys. Lett.* 33, 1020 (1978).
24. Chin-An Chang, R. Ludeke, L. L. Chang and L. Esaki, *Appl. Phys. Lett.* 31, 759 (1977).
25. S. Kishino, H. Nabashima, N. Chinone and R. Ito, *Appl. Phys. Lett.* 28, 98 (1976).
26. A. Y. Cho, *J. Appl. Phys.* 41, 2780 (1970).
27. R. Lukeke, L. Esaki and L. L. Chang, *Appl. Phys. Lett.* 24, 417 (1974).
28. A. Y. Cho, *J. Appl. Phys.* 46, 1733 (1975).
29. A. Y. Cho, R. W. Dixon, H. C. Casey, Jr. and R. L. Hartman, *Appl. Phys. Lett.* 28, 501 (1976).
30. A. Y. Cho, J. V. DiLorenzo, B. S. Hewitt, W. C. Niehaus and W. D. Schlosser, *J. Appl. Phys.* 48, 346 (1977).
31. W. C. Ballamy and A. Y. Cho, *IEEE Trans. Electron Devices* ED-23, 481 (1976).
32. A. Y. Cho, W. C. Ballamy, C. N. Dunn, R. L. Kuvas and W. E. Schroeder, *IEEE Trans. Electron Devices* ED-22, 248 (1975).
33. J. P. van der Ziel and M. Hlegems, *Appl. Opt.* 15, 1256 (1976).
34. J. L. Merz and A. Y. Cho, *Appl. Phys. Lett.* 28, 456 (1976).
35. J. L. Merz, R. A. Logan, W. Wiegmann and A. C. Gossard, *Appl. Phys. Lett.* 26, 337 (1975).
36. J. N. Walpole, A. R. Calawa, T. C. Harman and S. H. Groves, *Appl. Phys. Lett.* 28, 552 (1976).

37. R. W. Ralston, J. N. Walpole, T. C. Harman and I. Melngailis, *Appl. Phys. Lett.* 26, 64 (1975).
38. J. N. Walpole, A. R. Calawa, S. R. Chinn, S. H. Groves and T. C. Harman, *Appl. Phys. Lett.* 29, 307 (1976)
39. The effect of the carrier gas in VPE growth of GaAs was studied by Y. Seki, J. Matsui and H. Watanabe, *J. Appl. Phys.* 47, 3374 (1976).
40. A. Y. Cho, M. B. Panish, I. Hayashi, in *Proc. of 3rd International Symposium on GaAs and Related Compounds* (Institute of Physics, London, 1970). p. 18.
41. T. B. Rymer, *Electron Diffraction*, Chapman and Hall, London (1970).
42. A. Y. Cho, *J. Appl. Phys.* 42, 2074 (1971).
43. See, for example, J. K. Roberts and A. R. Miller, *Heat and Thermodynamics*, Interscience Publishers, Inc., New York, p. 93 (1960).
44. J. R. Arthur, *J. Appl. Phys.* 39, 4032 (1968).
45. C. M. Wolfe, G. E. Stillman and J. O. Dimmock, *J. Appl. Phys.* 41, 504 (1970).
46. D. J. Ashen, P. J. Dean, D. T. J. Hurle, J. B. Mullin and A. M. White, *J. Phys. Chem. Solids* 36, 1041 (1975).
47. W. H. Koschel, S. G. Bishop and B. D. McCombe, *Solid State Comm.* 19, 521 (1976).
48. W. J. Turner, G. O. Pettit and N. G. Ainslie, *J. Appl. Phys.* 34, 3274 (1963).
49. A. M. White, P. J. Dean, D. J. Ashen, J. B. Mullin, M. Webb, B. Day and R. D. Greene, *J. Phys. C. Solid State Phys.* 6, L243 (1973).
50. D. C. Reynolds, R. J. Almassy, C. W. Litton, S. B. Nam and G. L. McCoy, *Inst. Phys. Conf. Ser. No. 33b*, Chapter 3, 129 (1977).
51. M. Ilegems, R. Dingle and L. W. Rupp, Jr., *J. Appl. Phys.* 7, 3059 (1975).
52. M. B. Panish and M. Ilegems, *Prog. in Solid State Chemistry*, 7, 39 (1972).
53. T. P. Pearsall and R. W. Hopson, *J. Appl. Phys.* 48, 4407 (1977).

V. BIOGRAPHY AND PUBLICATIONS OF PRINCIPAL INVESTIGATOR

Arthur R. Calawa was born in Nashua, New Hampshire in 1928. He received the B. S. and M. S. degrees in Physics from the University of New Hampshire in 1954 and 1956, respectively. During his graduate years he worked on a U. S. Air Force contract study of cosmic ray neutron densities. He co-authored a publication and reported through meeting speeches on the correlation of cosmic ray neutron densities with sun spot activity in 1954-1956. He is a member of the Physics Honor Society, Sigma Pi Sigma, and past president of the University of New Hampshire chapter.

From 1956 to date he has been involved in the research and development of semiconductor materials and devices. From 1956 through 1959 he was a group leader at Fansteel Metallurgical Corporation, responsible for the development and pilot production of power silicon diodes. In 1959 he became a member of the research staff of the Applied Physics Group at M. I. T. Lincoln Laboratory. Since that time he has been involved in the research and development of tunnel diodes in Ge, InSb, GaSb, GaAs, PbTe, PbS, and PbSe, and has investigated the electronic band structures of some of these materials through temperature and magnetic field effects on these devices. He contributed significantly to the development of the first high-sensitivity Pb-salt detectors and later to the discovery of the first infrared semiconductor diode lasers that emit in the wavelength region from 4 to 32 μm . He has been involved in research on optical properties of semiconductors for over fourteen years, using such pumping schemes as electron beam, optical and minority carrier injection. He has investigated the tuning of diode lasers using magnetic field, pressure and temperature. He has utilized the most advanced semiconductor device technology, and recently developed techniques for the fabrication of sub-micron gratings on Pb-salt crystals. Most of his work has been reported in a number of meeting speeches, seminars, invited talks, and over 35 publications. His most recent work has been on the design and operation of one of the few existing molecular-beam crystal growth systems.

The following is a representative list of Mr. Calawa's publications.

Publications List -- A. R. Calawa

- "Magneto-Tunneling in InSb," A. R. Calawa, R. H. Rediker, B. Lax and A. L. McWhorter, *Phys. Rev. Lett.* 5, 55 (1960).
- "Magnetotunneling in Lead Telluride," R. H. Rediker and A. R. Calawa, *J. Appl. Phys.* 32, 2189 (1961).
- "Injection Electroluminescence in Gallium Antimonide," A. R. Calawa, *J. Appl. Phys.* 34, 1660 (1963).
- "Infrared InSb Laser Diode in High Magnetic Fields," R. J. Phelan, Jr., A. R. Calawa, R. H. Rediker, R. J. Keyes, and B. Lax, *Appl. Phys. Lett.* 3, 143 (1963).
- "PbTe Diode Laser," J. F. Butler, A. R. Calawa, R. J. Phelan, Jr., T. C. Harman, A. J. Strauss, and R. H. Rediker, *Appl. Phys. Lett.* 5, 75 (1964).
- "PbSe Diode Laser," J. F. Butler, A. R. Calawa, R. J. Phelan, Jr., A. J. Strauss, and R. H. Rediker, *Solid State Communications* 2, 303 (1964).
- "Properties of the PbSe Diode Laser," J. F. Butler, A. R. Calawa, and R. H. Rediker, *IEEE J. Quantum Electronics* QE-1, 4 (1965).
- "Electron Beam Pumped Lasers of PbS, PbSe, and PbTe," C. E. Hurwitz, A. R. Calawa, and R. H. Rediker, *IEEE Trans Quantum Electronics* QE-1, 102 (1965).
- "PbS Diode Laser," J. F. Butler and A. R. Calawa, *J. Electrochem. Soc.* 112, 2560 (1965).
- "Pressure-Tuned PbSe Diode Laser," J. M. Besson, J. F. Butler, A. R. Calawa, W. Paul, and R. H. Rediker, *Appl. Phys. Lett.* 7, 206 (1965).
- "Solution Regrowth of Planar InSb Laser Structures," I. Melngailis and A. R. Calawa, *J. Electrochem. Soc.* 113, 58 (1966).
- "Photovoltaic Effect in $Pb_xSn_{1-x}Te$ Diodes," I. Melngailis and A. R. Calawa, *Appl. Phys. Lett.* 9, 304 (1966).
- "Diode Lasers of $Pb_{1-y}Sn_ySe$ and $Pb_{1-x}Sn_xTe$," J. F. Butler, A. R. Calawa, and T. C. Harman, *Appl. Phys. Lett.* 9, 427 (1966).
- "Crystal Growth, Annealing, and Diffusion of Lead-Tin Chalcogenides," A. R. Calawa, T. C. Harman, M. Finn, and P. Youtz, *Trans. Met. Soc. AIME* 242, 374 (1968).
- "Tuning of PbSe Lasers by Hydrostatic Pressure from 8 to 22 μ ," J. M. Besson, W. Paul and A. R. Calawa, *Phys. Rev.* 173, 699 (1968).
- "Temperature and Compositional Dependence of Laser Emission in $Pb_{1-x}Sn_xSe$," T. C. Harman, A. R. Calawa, I. Melngailis, and J. O. Dimmock, *Appl. Phys. Lett.* 14, 333 (1969).

- "Magnetic Field Dependence of Laser Emission in $Pb_{1-x}Sn_xSe$ Diodes," A. R. Calawa, J. O. Dimmock, T. C. Harman, and I. Melngailis, *Phys. Rev. Lett.* 23, 7 (1969).
- "Interdiffusion in Lead Selenide," R. W. Brodersen, J. N. Walpole, and A. R. Calawa, *J. Appl. Phys.* 41, 1484 (1970).
- "Preparation and Properties of $Pb_{1-x}Cd_xS$," A. R. Calawa, J. A. Mroczkowski, and T. C. Harman, *J. Electronic Mat.* 1, (1972).
- "Tunable-Laser Spectroscopy of the ν_1 Band of SO_2 ," E. D. Hinkley, A. R. Calawa, P. L. Kelley, and S. A. Clough, *J. Appl. Phys.* 43, 3222 (1972).
- " $Pb_{1-x}Sn_xTe$ Photovoltaic Diodes and Diode Lasers Produced by Proton Bombardment," J. P. Donnelly, A. R. Calawa, T. C. Harman, A. G. Foyt, and W. T. Lindley, *Solid-State Electronics* 15, 403 (1972).
- "Small Bandgap Lasers and Their Uses in Spectroscopy," A. R. Calawa, *J. Luminescence* 7, 477 (1973).
- "High-Power Output in $Pb_{1-x}Sn_xTe$ Diode Lasers with Improved Mirror Quality," J. N. Walpole, A. R. Calawa, R. W. Ralston, and T. C. Harman, *J. Appl. Phys.* 44, 2905 (1973).
- "Single Heterojunction $Pb_{1-x}Sn_xTe$ Diode Lasers," J. N. Walpole, A. R. Calawa, R. W. Ralston, T. C. Harman, and J. P. McVittie, *Appl. Phys. Lett.* 23, 620 (1973).
- "Stripe-Geometry $Pb_{1-x}Sn_xTe$ Diode Lasers," R. W. Ralston, I. Melngailis, A. R. Calawa, and W. T. Lindley, *IEEE J. Quantum Electronics* QE-9, 350 (1973).
- "High cw Output Power in Stripe-Geometry PbS Diode Lasers," R. W. Ralston, J. N. Walpole, A. R. Calawa, T. C. Harman, and J. P. McVittie, *J. Appl. Phys.* 45, 1323 (1974).
- "Double-Heterostructure $PbSnTe$ Lasers Grown by Molecular-Beam Epitaxy with cw Operation up to 114 K," J. N. Walpole, A. R. Calawa, T. C. Harman, and S. H. Groves, *Appl. Phys. Lett.* 28, 552 (1976).
- "Distributed Feedback $Pb_{1-x}Sn_xTe$ Double-Heterostructure Lasers," J. N. Walpole, A. R. Calawa, S. R. Chinn, S. H. Groves, and T. C. Harman, *Appl. Phys. Lett.* 29, 307 (1976).
- "CW Operation of Distributed Feedback $Pb_{1-x}Sn_xTe$ Lasers," J. N. Walpole, A. R. Calawa, S. R. Chinn, S. H. Groves, and T. C. Harman, *Appl. Phys. Lett.* 30, 524 (1977).
- "Effect of H_2 on Residual Impurities in GaAs MBE Layers," A. R. Calawa, *Appl. Phys. Lett.* 33, 1020 (1978).

UNCLASSIFIED

SECURITY CLASSIFICATION OF THIS PAGE (When Data Entered)

REPORT DOCUMENTATION PAGE		READ INSTRUCTIONS BEFORE COMPLETING FORM
1. REPORT NUMBER ESD-TR-78-397 ✓	2. GOVT ACCESSION NO.	3. RECIPIENT'S CATALOG NUMBER (9)
4. TITLE (and Subtitle) (6) GaInAs and GaInAsP MBE Crystal Growth	5. TYPE OF REPORT & PERIOD COVERED Annual Report, 1 May 1977 - 30 April 1978	
7. AUTHOR(s) (10) Arthur R. Calawa	8. CONTRACT OR GRANT NUMBER(s) (15) F19628-78-C-0002 ✓	
9. PERFORMING ORGANIZATION NAME AND ADDRESS Lincoln Laboratory, M.I.T. ✓ P.O. Box 73 Lexington, MA 02173	10. PROGRAM ELEMENT, PROJECT, TASK AREA & WORK UNIT NUMBERS Program Element No. 61102F	
11. CONTROLLING OFFICE NAME AND ADDRESS Air Force Systems Command, USAF Andrews AFB Washington, DC 20331	12. REPORT DATE (11) 30 April 1978	13. NUMBER OF PAGES
14. MONITORING AGENCY NAME & ADDRESS (if different from Controlling Office) Electronic Systems Division Hanscom AFB Bedford, MA 01731 (12) 530	15. SECURITY CLASS. (of this report) Unclassified	
15a. DECLASSIFICATION DOWNGRADING SCHEDULE		
16. DISTRIBUTION STATEMENT (of this Report) Approved for public release; distribution unlimited.		
17. DISTRIBUTION STATEMENT (of the abstract entered in Block 20, if different from Report)		
18. SUPPLEMENTARY NOTES None		
19. KEY WORDS (Continue on reverse side if necessary and identify by block number)		
MBE GaInAsP films	InP substrates hydrogen growth technique	
20. ABSTRACT (Continue on reverse side if necessary and identify by block number)		
<p>The most important result of the first year of this program is our discovery that the introduction of hydrogen during the growth of GaAs films by molecular beam epitaxy (MBE) brings about a dramatic improvement in the electrical characteristics of these films. In addition to providing a major advance in the growth of similiarly high quality GaInAs and GaInAsP films on InP substrates, the long range goals of this program.</p> <p>In addition to discovering, understanding, and optimizing the hydrogen growth technique, we have also grown GaInAs films on InP substrates, and have considered possible techniques for controlling the As to P ratio for GaInAsP layer growth.</p>		

207650

LB

20. ABSTRACT (Continued)

Prior to the development of the hydrogen technique, several growths of GaAs on GaAs were completed in order to identify and eliminate sources of impurities from the MBE system. For n-type layers with carrier concentrations in excess of 10^{17} cm^{-3} the electrical characteristics appeared normal but as the carrier concentration was reduced below 10^{17} cm^{-3} the increase in 77 K mobility normally observed was not seen. This is expected if the ionized impurity concentration remains in the range of $5 \times 10^{16} \text{ cm}^{-3}$ to 10^{17} cm^{-3} . After a careful review of the literature,¹⁻⁸ it became apparent that very little 77 K mobility data on MBE layers was available and that nearly all of the published data agreed with our results.⁷ Only one published 77 K mobility value¹ was significantly higher than all the others and there is no indication of its reproducibility. This large number of compensating impurities would significantly reduce the electron drift velocity in these materials, an effect which is detrimental to microwave devices. The use of hydrogen during growth, described in detail in this report, significantly reduces the carrier compensation due to residual impurities and results in much higher electron mobilities. Results of photoluminescence measurements on these materials are given which tentatively identify the important residual impurities in MBE grown GaAs as due to carbon and oxygen.

In addition to the development of GaAs MBE growth, we have begun development of GaInAs growth and initial results of the growth of GaInAs layers on InP substrates are given. In particular, procedures are described by which uniform, homogeneous layers of GaInAs can be grown over large area substrates by precisely controlling the In/Ga ratio. Finally, consideration is given to the control of the As/P ratio for the MBE growth of GaInAsP on InP substrates.